invasion, extrahepatic metastasis or Child–Pugh score C) and death as an absorbing state from where no transitions to the other states occurred. The model was based on the following principles: (i) the four states are mutually exclusive and collectively exhaustive; (ii) the Markov assumption for the current state without any memories of prior states; (iii) time intervals are uniform; and (iv) transition probabilities are constant and time independent. Items (i) and (ii) define a Markov chain, whereas items (iii) and (iv) characterize a homogenous Markov chain (18).

A $P$-value of $< 0.05$ in a two-tailed test was considered significant. Data analysis was performed using the computer program IBM SPSS STATISTICS ver. 18 (19).

## Results

### Effect of initial treatment

After the initial session of RFA or surgery, complete ablation for entire tumour nodules was obtained in 232 patients (98.3%) in the RFA group and in 138 patients (100%) in the surgery group. Among four patients (1.7%) with incomplete ablation after the initial session of RFA, two achieved complete necrosis by re-RFA performed after a few months, and the other two underwent TACE for the residual tumour nodules.

### Complications of treatment (Table 2)

After the initial therapy with RFA or surgery, 12 patients developed major complications after treatment: seven in the RFA group and five in the surgery group. There was no treatment-related death within 6 months after therapy in any of the patients in the RFA and surgery groups. Although abdominal pain, mild aggravation of liver function test, low-grade fever, transient elevation of aminotransferases and bilirubin values were often found after RFA therapy, significant deterioration of performance status and prolonged stay in the hospital were not observed.

### Cumulative recurrence rates and treatment for recurrent hepatocellular carcinoma

The initial recurrence rates were compared between the two groups according to the initial therapy. The initial recurrence rates after treatment in the RFA and the surgery group were 11.3 and 14.2% at the end of the first year, 40.4 and 29.3% in the second year, 53.3 and 40.6% in the third year, 65.0 and 48.8% in the fourth year and 69.5 and 53.7% in the fifth year respectively. The recurrence rate in the RFA group was significantly higher than that of the surgery group (log-rank test, $P = 0.015$) (Fig. 2).

For the treatment of a recurrent tumour, we fundamentally adopted RFA or surgical treatment when patients had an early stage of HCC with sufficient liver function. Although initial therapy included surgery, patients with a recurrent tumour tended to receive RFA therapy more frequently. When a tumour progressed to the intermediate stage with a large tumour and/or multiple nodules, TACE was usually performed using anti-tumour agents, iodinated poppy seed oil fatty acid (Lipiodol Ultra-Fluide$^{TM}$, Guerbet Japan, Tokyo) and gelatin sponge particles. When the tumour progressed to the advanced stage (portal invasion, extrahepatic metastasis, or Child–Pugh C) during repeated local ablation or TACE therapy, anti-tumour therapy was usually not performed, except for systemic or intra-arterial chemotherapy. Anti-molecular targeted agents were not available during the study period in Japan.

**Table 2.** Complications after the initial treatment

| Complication | Initial therapy: Radiofrequency ablation ($n = 236$) | Initial therapy: Hepatic resection ($n = 138$) |
|---|---|---|
| Perforation of jejunum | 2 | 0 |
| Biloma and/or biliary infection | 3 | 1 |
| Prolonged ascites | 1 | 2 |
| Jaundice | 0 | 1 |
| Haemorrhage requiring transfusion | 1 | 1 |

### Cumulative progression rates from the early to the intermediate stage

A total of 98 (26.2%) developed to the intermediate stage during the observation: 65 (27.5%) in the RFA group and 33 (23.9%) in the surgery group.

Crude development rates to the intermediate stage in the RFA and surgery groups were 18.2 and 13.0% in the third year, 33.1 and 22.1% in the fifth year, and 40.9 and 31.8% in the fifth year respectively. The development rate of the RFA group was slightly higher ($P = 0.14$) (Fig. 3a).

Independent factors associated with the stage development rate were explored in the patients. Multivariate hazard analysis showed that the rate is independently associated with positive HBsAg ($P = 0.041$) and a high platelet count ($P = 0.032$). The factor of initial therapy

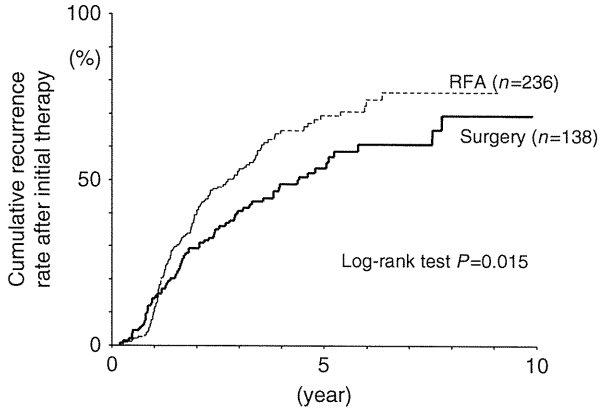


**Fig. 2.** Cumulative recurrence rates after therapy in patients with an early stage of hepatocellular carcinoma, according to initial therapy. RFA, radiofrequency ablation.

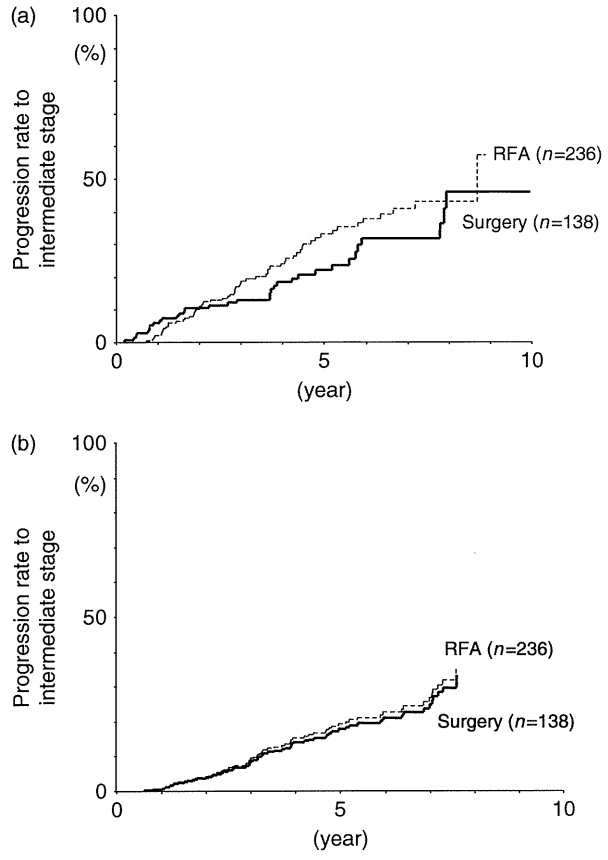


**Fig. 3.** (a) Crude development rates to the intermediate stage of hepatocellular carcinoma according to initial therapy. (b) Adjusted development rates to the intermediate stage, using proportional hazard analysis. RFA, radiofrequency ablation.

did not affect the eventual survival rate (hazard ratio 1.09, $P = 0.70$) (Table 3).

Cumulative progression curves from the early stage to the intermediate stage were drawn from the multivariate analysis in an imaginary RFA group and an imaginary surgery group, with an average positive rate of HBsAg and an average platelet count (Fig. 3b). Five-year progression rates to the intermediate stage were 19% in the RFA group and 18% in the surgery group. The differences in the progression rates were considered as a 'pure' impact of the difference in the initial mode of therapy on future stage progression, which was adjusted with significant covariates assuming a standardized study group.

### Survival rates and predictive factors

A total of 87 (23.3%) died during the observation: 60 (25.4%) in the RFA group and 27 (19.6%) in the surgery group.

The crude survival rates in the RFA group and the surgery group were 88.5 and 92.6% in the third year, 71.7 and 80.9% in the fifth year and 60.6 and 74.6% in the seventh year respectively (Fig. 4a). The survival rate of the surgical therapy group was higher but statistical significance was not obtained ($P = 0.071$).

**Table 3.** Independent factors associated with the progression rate from an early stage to an intermediate stage of hepatocellular carcinoma

| Factors | Category | Hazard ratio (95% confidence interval) | *P* |
|---|---|---|---|
| HBsAg | 1: negative | 1 | |
| | 2: positive | 0.41 (0.20–0.82) | 0.012 |
| Platelet count | 1: ≥ 100 000/mm$^3$ | 1 | |
| | 2: < 100 000/mm$^3$ | 1.58 (1.04–2.39) | 0.032 |
| Initial therapy | 1: surgery | 1 | |
| | 2: RFA | 1.09 (0.69–1.71) | 0.70 |

RFA, radiofrequency ablation.

Independent factors associated with survival were explored in all the patients. Multivariate hazard analysis indicated that the survival rate is independently associated with a positive HBsAg ($P = 0.038$), a low indocyanine green retention rate at 15 min (ICG R15) ($P < 0.001$) and a low AFP value ($P = 0.021$). The factor of initial therapy did not affect the eventual survival rate (hazard ratio 1.26, $P = 0.35$) (Table 4).

Overall survival curves in patients with an early stage of HCC were drawn from the multivariate analysis in an imaginary RFA group and an imaginary surgery group, using an average positive rate of HBsAg, an average ICG R15 value and an average AFP value (Fig. 4b). Five-year survival rates were estimated as 80% in the RFA group and 81% in the surgery group, and 7-year rates were 71 and 72% respectively. Among 87 deaths during the observation, 70 (80.5%) died from progression of HCC, 14 (16.1%) died from liver failure without progression of HCC and the remaining three patients died from causes other than liver disease

### Probabilities for transition among four disease states of hepatocellular carcinoma

The Markov model for the progression of HCC depended on the probabilities for transition among the four states at one time interval that was set at 1 year. Yearly transition probabilities were calculated based on 1892 person-year data from the 374 patients with an early stage of HCC. Figure 5 illustrates a probability diagram of the long-term progression of HCC calculated from the Markov model. All patients were at an early stage initially, but intermediate and advanced stages gradually increased with time. Approximately half of the patients died, and < 40% of the patients remained at early stage at the end of the 10th year.

The results are shown in Table 5 as a matrix of the transition probabilities for three subsets composed of three decades of their lives (< 60, 60–69 and ≥ 70 years) stratified by four states (early stage, intermediate stage, advanced stage and death).

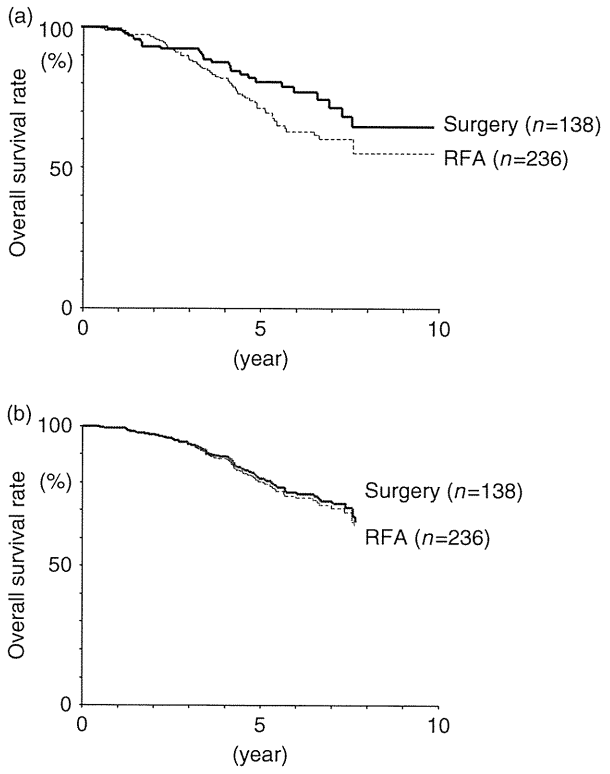


**Fig. 4.** (a) Crude survival rates in patients receiving radiofrequency ablation and those undergoing surgery as the initial therapy. (b) Adjusted survival rates in the radiofrequency group and surgery group, using proportional hazard analysis. RFA, radiofrequency ablation.

**Table 4.** Independent factors associated with the survival rate after the initial treatment for hepatocellular carcinoma

| Factors | Category | Hazard ratio (95% confidence interval) | *P* |
|---|---|---|---|
| HBsAg | 1: negative | 1 | |
| | 2: positive | 0.43 (0.19–0.94) | 0.034 |
| ICG R15* | 1: < 30% | 1 | |
| | 2: ≥30% | 1.96 (1.20–3.20) | 0.0070 |
| α-fetoprotein | 1: < 40 mg/ml | 1 | |
| | 2: ≥40 mg/ml | 1.71 (1.09–2.68) | 0.020 |
| Prothrombin time | 1: < 80% | 1 | |
| | 2: ≥80% | 0.60 (0.37–0.96) | 0.035 |
| Initial therapy | 1: surgery | 1 | |
| | 2: RFA | 1.09 (0.66–1.81) | 0.73 |

*ICG R15, indocyanine green retention rate at 15 min.
RFA, radiofrequency ablation.

In the matrix of age of < 60 years, 2.34% of the patients in the early stage developed to the intermediate stage annually, 1.40% to the advanced stage and 0.93% died. The remaining 95.33% of the patients remained in the early stage after 1 year. The probability for the transition from an early stage to an intermediate stage

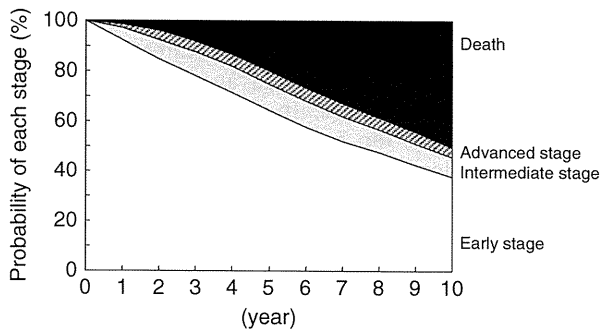


**Fig. 5.** Illustrated transition probabilities of patients, from the early stage of hepatocellular carcinoma, to the intermediate stage, the advanced stage and to death.

**Table 5.** One-year state-transition probability matrices for subsets of hepatocellular carcinoma*

| | Early | Intermediate | Advanced | Death |
|---|---|---|---|---|
| All Patients of all age groups | | | | |
| Early | 92.17 | 4.81 | 1.73 | 1.29 |
| Intermediate | | 69.32 | 27.27 | 3.41 |
| Advanced | | | 24.77 | 75.23 |
| Death | | | | 100.00 |
| Age < 60 years | | | | |
| Early | 95.33 | 2.34 | 1.40 | 0.93 |
| Intermediate | | 58.33 | 37.50 | 4.17 |
| Advanced | | | 23.53 | 76.47 |
| Death | | | | 100.00 |
| Age 60–69 years | | | | |
| Early | 91.40 | 5.90 | 1.35 | 1.35 |
| Intermediate | | 68.18 | 30.30 | 1.52 |
| Advanced | | | 22.21 | 78.79 |
| Death | | | | 100.00 |
| Age ≥70 years | | | | |
| Early | 90.68 | 5.49 | 2.33 | 1.50 |
| Intermediate | | 74.42 | 22.09 | 3.49 |
| Advanced | | | 27.91 | 72.09 |
| Death | | | | 100.00 |

*Early stage, solitary or multiple up to three nodules 3 cm or less each; Intermediate stage, four nodules or more, or larger than 3 cm; Advanced stage, portal vein invasion, extrahepatic metastasis, or Child–Pugh score C.

was significantly lower in young patients < 60 years of age (2.34%) than that in patients 60 years of age or older (5.70%)($\chi^2 = 7.76$, $P = 0.0053$). From the matrix stratified by three age groups, the transition probability from an intermediate to an advanced stage decreased with age: 37.50% in patients < 60 year of age, 30.30% in patients 60–69 year of age and 22.09% in patients 70 year of age or older ($\chi^2 = 10.57$, $P = 0.0011$).

### Probabilities for transition according to the initial treatment

We also evaluated the transition probabilities among the four states in the subgroups of RFA and surgery as the initial mode of therapy.

In the matrix of patients receiving RFA therapy, the transition probability from early to intermediate stage was 5.40%, probability to the advanced stage was 1.63% and to death was 1.73%. In the patients undergoing surgery, the transition probability from an early to an intermediate stage was 3.90%, probability to an advanced stage was 1.87% and to death was 0.62%.

The probability for the transition from an early stage to an intermediate stage was slightly higher in the RFA group (5.40%) than that in the surgery group (3.90%), but statistical significance was not found ($\chi^2 = 1.90$, $P = 0.17$).

## Discussion

Radiofrequency ablation has been considered as a less curative mode of therapy than surgical resection, because local tumour progression sometimes occurs after conservative treatment with relatively small ablative margins. As those patients with loco-regional therapy are generally followed up for tumour recurrence with a short time interval of 3–6 months using CT or MRI, we can usually ablate a newly appeared or a locally progressed tumour within a small size and few numbers. In order to elucidate the efficacies and usefulness of RFA compared with surgical resection, we analysed many HCC patients receiving RFA or surgical therapy regarding tumour progression and survival.

Fortunately, in Japan, where highly socialized medicine is practiced with everyone covered by some form of health insurance, almost all of the patients can receive any extensive medical services including surgery, RFA, embolization and repeated imaging diagnosis, regardless of the cost. Under intensive check-up and treatment repetition, the Markov model showed the probability of remaining at the early stage as 92.17% per year: the transition rate from the early to the intermediate stage was 4.81%, to the advanced stage 1.73 and to death 1.29% respectively. Similarly, the probabilities of remaining at the intermediate and advanced stages were 69.32 and 24.77% per year respectively.

Because young patients with HCC usually have better liver function and a relatively low carcinogenesis rate, younger patients are more likely to undergo radical methods of therapy for a recurrent tumour repeatedly. The reason for the low transition rate from the early to the intermediate stage was convincingly explained in the young patient group (Table 4). In contrast, the transition rate from the intermediate to the advanced stage was significantly higher in the young patient group. Although the exact reason was not known, multiple tumours of younger patients possibly progressed rapidly or were resistant to TACE. Hence, the Markov model would be eligible for simulating the outcomes of patients with the early stage of HCC. It is also helpful in planning strategies for the management of small HCC, for the eventual prolongation of a patient's life and for ideal cost-effective guidelines on a national basis, not only in Japan but also elsewhere in the world where the prevalence of HCC is increasing. Although we once generated a 'five-state model' consisting of no tumour, early stage, intermediate stage, advanced stage and death, we finally adopted the current 'four-state model' because of good mathematical fit and statistical robustness. Molinari and Helton (20) and Cho *et al.* (21) described a progression model of HCC after RFA and/or hepatectomy by the Markov model. Both authors performed a meta-analysis-like study using heterogeneous sources of patients from varied published articles, and estimated progression models of HCC in hypothetical patient cohorts. We analysed the actual clinical courses of patients in a single institution, where the same diagnostic and therapeutic procedures were adopted for every patient. Sufficient medical procedures and resources under a universal medical insurance system of the country seemed to give rise to better outcomes and survival, but an exact comparison cannot be carried out using the current data and the previous literatures.

In this study, we also compared RFA and surgery as an initial therapy for the early stage of HCC. Understandably, older patients, patients with severe cirrhosis and those with a concomitant disease other than liver disease tended to undergo non-surgical therapy. In addition, young patients with HBV-related HCC were likely to receive surgery because of good liver function, relatively low potential of recurrence and young age. Although the crude recurrence rate and the crude progression rate from the early stage to the intermediate stage were higher in patients receiving RFA therapy, multivariate analysis with adjustment of background biases showed that the initial mode of therapy did not affect the progression rate and did not affect the overall survival rate. When a regular check-up of imagings with an interval of 3–4 months was conducted, an additional ablation therapy was usually performed successfully for a small locally progressed tumour. Under intensive medical care for liver disease, the initial mode of therapy therefore did not affect the overall survival of a patient with an early stage of HCC. When a careful check-up with imagings and adequate application of repeated ablative procedures for HCC were performed, the choice of ablative manners was insignificant compared with the background liver features of aetiology of liver disease (hepatitis virus) and severity of liver disease (platelet count). The choice of ablative therapy for small-sized HCC should also be assessed from the viewpoints of conservation of liver function, cost-effectiveness and quality of life (9, 10, 12, 22).

Since it seemed to require at least 5 years to obtain a statistical difference in the recurrence rates and survival rates between RFA-treated and surgically treated groups, a prospective randomized trial is actually difficult to perform from both ethical and medical viewpoints. One of the significant results of the current study is that highly socialized medical circumstances with sufficient medical practice can attain a high survival rate of 71–80% at the end of the fifth year in patients at an early stage.

Further studies are required to determine the relationship between patient's age and stage transition. Because HCV-related chronic hepatitis often progresses to HCC during the clinical course, this kind of staging model with analyses of medical intervention will be necessary in the future from the viewpoints of epidemiological assessment and medical politics, together with patient's quality of life and feeling of satisfaction.

## Acknowledgements

This study was supported in part by a research grant from the Ministry of Health, Labor and Welfare, Japan.

*Financial Disclosure*: We have no financial relationships with any commercial pharmaceutical companies, biochemical device manufacturers or other corporations whose products or services are related to the subject matter of the presentation topic.

## References

1. Sherman M. Hepatocellular carcinoma: epidemiology, surveillance, and diagnosis. *Semin Liver Dis* 2010; **30**: 3–16.
2. Ikai I, Yuji I, Okita M, *et al.* Report of the 15th follow-up survey of primary liver cancer. The liver cancer study group of Japan. *Hepatol Res* 2004; **28**: 21–9.
3. Ikai I, Arii S, Ichida T, *et al.* Report of the 16th follow-up survey of primary liver cancer. The liver cancer study group of Japan. *Hepatol Res* 2005; **32**: 163–72.
4. Kim WR, Gores GJ, Benson JT, Therneau TM, Melton LJ III. Mortality and hospital utilization for hepatocellular carcinoma in the United States. *Gastroenterology* 2005; **129**: 486–93.
5. El-Serag HB, Siegel AB, Davila JA, *et al.* Treatment and outcomes of treating of hepatocellular carcinoma among Medicare recipients in the United States: a population-based study. *J Hepatol* 2006; **44**: 158–66.
6. Ikeda K, Arase Y, Kobayashi M, *et al.* Significance of multicentric cancer recurrence after potentially curative ablation of hepatocellular carcinoma: a longterm cohort study of 882 patients with viral cirrhosis. *J Gastroenterol* 2003; **38**: 865–76.
7. Ueno S, Aoki D, Maeda T, *et al.* Preoperative assessment of multicentric occurrence in synchronous small and multiple hepatocellular carcinoma based on image-patterns and histological grading of non-cancerous region. *Hepatol Res* 2004; **29**: 24–30.
8. Wang J, Li Q, Sun Y, *et al.* Clinicopathologic features between multicentric occurrence and intrahepatic metastasis of multiple hepatocellular carcinomas related to HBV. *Surg Oncol* 2009; **18**: 25–30.
9. Livraghi T, Meloni F, DiStasi M, *et al.* Sustained complete response and complications rates after radiofrequency ablation of very early hepatocellular carcinoma in cirrhosis: is resection still the treatment of choice? *Hepatology* 2008; **47**: 82–9.
10. Ikeda K, Kobayashi M, Saitoh S, *et al.* Cost-effectiveness of radiofrequency ablation and surgical therapy for small hepatocellular carcinoma of 3 cm or less in diameter. *Hepatol Res* 2005; **33**: 241–9.
11. Chen MS, Li JQ, Zheng Y, *et al.* A prospective randomized trial comparing percutaneous local ablative therapy and partial hepatectomy for small hepatocellular carcinoma. *Ann Surg* 2006; **243**: 321–8.
12. Guglielmi A, Ruzzenente A, Valdegamberi A, *et al.* Radiofrequency ablation versus surgical resection for the treatment of hepatocellular carcinoma in cirrhosis. *J Gastrointest Surg* 2008; **12**: 192–8.
13. Ogihara M, Wong LL, Machi J. Radiofrequency ablation versus surgical resection for single nodule hepatocellular carcinoma: long-term outcomes. *HPB* 2005; **7**: 214–21.
14. Chen MS, Li JQ, Zheng Y, *et al.* A Prospective randomized trial comparing percutaneous local ablative therapy and partial hepatectomy for small hepatocellular carcinoma. *Ann Surg* 2006; **243**: 321–8.
15. Llovet JM, Bru C, Bruix J. Prognosis of hepatocellular carcinoma: BCLC staging classification. *Semin Liver Dis* 1999; **19**: 329–38.
16. Kaplan EL, Meier P. Nonparametric estimation for incomplete observation. *J Am Stat Assoc* 1958; **53**: 457–81.
17. Beck JR, Pauker SG. The Markov process in medical prognosis. *Med Decis Making* 1983; **3**: 419–58.
18. Silverstein MD, Albert DA, Hadler NM, Ropes MW. Prognosis of SLE: comparison of Markov model to life table analysis. *J Clin Epidemiol* 1988; **41**: 623–33.
19. IBM SPSS Inc. *IBM SPSS for Windows version 18.0 Manual.* Armonk, NY, USA: SPSS Japan Inc., an IBM company, 2009.
20. Molinari M, Helton S. Hepatic resection versus radiofrequency ablation for hepatocellular carcinoma in cirrhosis individuals not candidates for liver transplantation: a Markov model decision analysis. *Am J Surg* 2006; **198**: 396–406.
21. Cho YK, Kim JK, Kim WT, Chung JW. Hepatic resection versus radiofrequency ablation for very early stage hepatocellular carcinoma: a Markov model analysis. *Hepatology* 2010; **51**: 1284–90.
22. Lau WY, Lai EC. The current role of radiofrequency ablation in the management of hepatocellular carcinoma: a systematic review. *Ann Surg* 2009; **249**: 20–5.

# Heterogeneous Type 4 Enhancement of Hepatocellular Carcinoma on Dynamic CT Is Associated With Tumor Recurrence After Radiofrequency Ablation

Yusuke Kawamura[1]
Kenji Ikeda
Yuya Seko
Tetsuya Hosaka
Masahiro Kobayashi
Satoshi Saitoh
Hiromitsu Kumada

**OBJECTIVE.** The aim of this study was to predict recurrence of hepatocellular carcinoma (HCC) from baseline dynamic CT images.

**MATERIALS AND METHODS.** This retrospective study included 191 consecutive patients who underwent surgical resection or radiofrequency ablation (RFA) between January 2005 and September 2009 for the treatment of HCC. Enhancement on pretreatment arterial and portal phase dynamic CT images was classified into one of the four following enhancement patterns: Types 1 and 2 are homogeneous enhancement patterns without or with increased arterial blood flow, respectively; type 3 is a heterogeneous enhancement pattern with septations; and type 4 is an irregularly shaped ring structure enhancement pattern. Predictive factors for tumor recurrence including dynamic CT enhancement pattern were also evaluated. Moreover, risk factors including recurrence type (i.e., tumor number ≥ 10, portal vein invasion, or both) were evaluated in RFA-treated cases.

**RESULTS.** Among 60 patients who underwent surgical resection, no statistical association was observed between dynamic CT enhancement patterns and recurrence rate. In contrast, in the 131 patients who underwent RFA, cumulative recurrence rates for each enhancement pattern were significantly different: Recurrence rates 2 years after RFA for patients with type 1, 2, 3, and 4 were 26.6%, 46.9%, 38.6%, and 77.8%, respectively ($p = 0.042$). Recurrence, which was defined as the presence of 10 or more nodules, portal vein invasion, or both occurred in nine of 131 patients (6.9%) in the RFA group. A multivariate Cox proportional hazards analysis revealed that the type 4 dynamic CT enhancement pattern is an independent factor for HCC recurrence (hazard ratio, 27.68; 95% CI, 6.82–112.33; $p < 0.001$).

**CONCLUSION.** The pretreatment type 4 dynamic CT enhancement pattern can potentially be used to predict recurrence of HCC after RFA treatment.

**Keywords:** dynamic CT, hepatocellular carcinoma, radiofrequency ablation, recurrence, surgical resection

DOI:10.2214/AJR.11.6843

Received March 10, 2010; accepted after revision June 7, 2011.

Supported by the Okinaka Memorial Institute for Medical Research and Japanese Ministry of Health, Labour and Welfare.

[1]All authors: Department of Hepatology, Toranomon Hospital, 2-2-2, Toranomon, Minato-ku, Tokyo 105-8470, Japan. Address correspondence to Y. Kawamura (k-yusuke@toranomon.gr.jp).

**WEB**
This is a Web exclusive article.

*AJR* 2011; 197:W665–W673

0361–803X/11/1974–W665



Hepatocellular carcinoma (HCC) is a common malignancy worldwide, and the incidence rate is increasing in Japan as well as in the United States [1–3]. Chronic viral hepatitis and liver cirrhosis after infection with hepatitis B virus (HBV) and hepatitis C virus (HCV) play important roles in the development of HCC [4, 5]. The incidence of HCC in patients with HCV-related cirrhosis is estimated to be 5–10% per annum in Japan, and HCV-related cirrhosis is one of the major causes of death particularly in Asian countries [5]. Among the available treatment options for HCC, surgical resection is generally considered to be a local eradication method that can provide a satisfactory long-term outcome [6–13]. Advances in imaging procedures have led to the increased detection of early stage HCC and have improved survival because more patients in whom hepatic resection is possible are being identified [14, 15].

For patients who are not eligible for surgical treatment for various reasons (e.g., lack of sufficient liver function for surgical resection), percutaneous local therapy is a viable therapeutic option. A number of local ablation therapies are available including percutaneous ethanol injection, percutaneous acetic acid injection, cryotherapy, percutaneous microwave coagulation therapy, and radiofrequency ablation (RFA). In addition to surgical resection, local ablation therapies, particularly RFA, are considered to be local eradication methods for HCC that can provide good long-term outcomes [16]. However, despite the high complete necrosis rate in RFA-treated HCC, some patients experience tumor recurrence within 1 year of RFA, either as local recurrence or new tumor formation. A series of studies have

identified factors predictive of HCC tumor recurrence and seeding including tumor size, tumor location relative to the hepatic capsule (presence or absence of tumor on subcapsular portion), α-fetoprotein (AFP) level, tumor stage, and histopathologic grade [17, 18]. For the reasons stated earlier, it is important to determine the histopathologic grade of HCC before administering local ablation therapy.

We previously reported that a "heterogeneous enhancement pattern with irregular ring-like structures" [19] in the arterial phase of dynamic CT analysis accurately predicts the histopathologic grade of poorly differentiated HCC, and we named this enhancement pattern "type 4" [19]. Therefore, one aim of the current study was to examine the risk factors for tumor recurrence after local eradication, including differences between treatment procedure (surgical resection vs RFA) and dynamic CT enhancement pattern. Moreover, in a previous study, investigators reported an association between tumor seeding after RFA and histopathologic grade of HCC [17, 18]. Therefore, the other aim of the current study was to evaluate the relationship between the type 4 dynamic CT enhancement pattern and HCC recurrence in patients who undergo RFA.

## Materials and Methods

### Study Population

From January 2005 to September 2009, 705 patients were diagnosed with HCC and underwent surgical resection or RFA as the initial treatment in the Department of Hepatology, Toranomon Hospital, Tokyo, Japan. Among the 705 patients, 191 patients satisfied the following criteria for inclusion in our study: triple-phase dynamic CT study performed before surgical resection or RFA; pretreatment diagnosis of a solitary HCC with a maximum tumor diameter of 30 mm or less; no evidence of extrahepatic metastases as confirmed on pretreatment imaging studies (CT, sonography, or chest radiography); no history of other malignancies; and no pretreatment chemotherapy, including transcatheter arterial chemoembolization (TACE). Accordingly, these 191 patients were retrospectively evaluated for an association between arterial and portal phase dynamic CT enhancement pattern and recurrence of HCC. The observation starting point was the time of the first surgical resection or RFA session for HCC.

### Contrast Infusion and CT Protocol

All patients received nonionic contrast material with an iodine concentration of 350 mg I/mL (iomeprol [Iomeron 350, Bracco-Eisai]). CT was performed with a 64-MDCT scanner (Aquilion 64, Toshiba Medical Systems) with the following scanning parameters: rotation time, 0.5 second; beam collimation, 64 × 0.5 mm; section thickness and interval, 5 mm; beam pitch, 0.83; tube voltage, 120 kV; and tube current, 150 mAs. All helical scans were started at the top of the liver and proceeded in a cephalocaudal direction. Unenhanced and three-phase contrast-enhanced helical scans of the whole liver were obtained. Patients were instructed to hold their breath with exhalation during scanning.

An automatic bolus-tracking program (Sure Start, Toshiba Medical Systems) was used to time the start of acquisition in each phase after contrast injection. The attenuation at the axis of the celiac artery level was monitored by one radiology technician; the region-of-interest cursor (1 $cm^2$) was placed in the abdominal aorta. Real-time low-dose (120 kV, 25 mAs) serial monitoring studies were initiated 5 seconds after the start of contrast injection. The trigger threshold level was set at 100 HU. A double arterial phase acquisition was started 15 and 20 seconds after triggering, and portal phase and delayed phase acquisitions were started 70 and 180 seconds after the start of the contrast injection, respectively.

### Diagnosis of HCC

Diagnosis of HCC was predominantly based on image analysis. If a hepatic nodular lesion was identified on screening sonography, the patient underwent dynamic CT, dynamic MRI, or both. Furthermore, when a liver nodule either showed hyperattenuation in the arterial phase of the dynamic study and washout in the portal or delayed phase or showed typical hypervascular staining on digital subtraction angiography, the nodule was diagnosed as HCC. In accordance with the American Association for the Study of Liver Diseases guidelines [20], we obtained at least two dynamic images before treatment. When a nodule did not appear to show the mentioned typical imaging features, fine-needle aspiration biopsy was performed followed by histologic examination and diagnosis.

### Imaging Analysis of Hepatocellular Carcinoma and Definition of Enhancement Pattern

Before treatment was administered, triple-phase contrast-enhanced CT was performed of all patients. The enhancement pattern on the arterial and portal phases of dynamic CT was classified into one of four types, and the four enhancement types on the original images were converted into simplified images (Fig. 1 [19]). The type 1 pattern represented a homogeneous enhancement pattern with no increase in arterial blood flow; the entire image was uniform during the arterial phase and portal phase. The type 2 pattern represented a homogeneous enhancement pattern with increased arterial blood flow; the entire image was uniform during the arterial phase and portal phase. The type 3 pattern represented a heterogeneous enhancement pattern with septations with heterogeneous enhancement and septations in the arterial phase, whereas the septations resembled a near-uniform tumor tissue periphery in the portal phase. The type 4 pattern represented a heterogeneous enhancement pattern with irregular ring-like structures; the arterial phase was marked by the presence of irregularly shaped ring areas of enhancement and areas of little blood flow relative

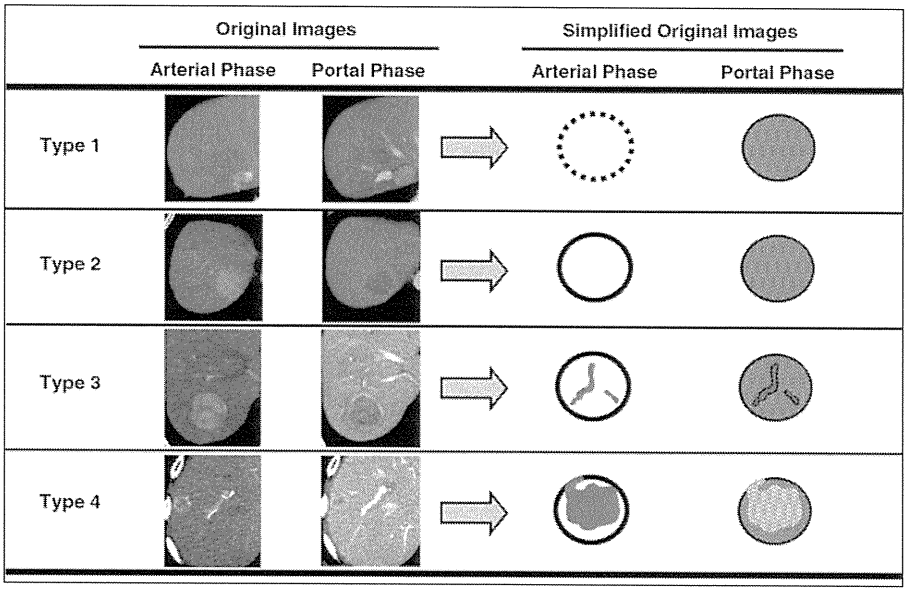


**Fig. 1**—Sample of original dynamic CT images and simplified images for each enhancement pattern. (Reprinted and modified with permission from John Wiley and Sons [19])

to the periphery of the tumor tissue, and the portal phase was characterized by areas of reduced blood flow.

The enhancement pattern on the arterial and portal phases of dynamic CT was determined by consensus of three expert hepatologists who were blinded to the pathologic results.

### *Treatment Methods*

Physicians and surgeons generally discussed the preferred choice of therapy in individual patients. Hepatic resection was performed under intraoperative sonographic monitoring and guidance. For small and superficial HCCs, arterial and portal vein clamping at the hepatic hilum was not usually required to maintain liver perfusion. RFA was performed using three different devices: a multitined expandable electrode with a 3-cm array with a 150-W radiofrequency generator (model 1500 series, RITA Medical Systems), an internally cooled electrode with a 3-cm active tip with a 200-W radiofrequency generator (Cool-tip Radiofrequency System, Covidien), and a multitined expandable electrode with a 200-W radiofrequency generator (LeVeen Needle Electrode and Radiofrequency 3000 Generator, RTC System, Boston Scientific Japan). For the first two systems, treatment procedures were performed according to the protocols recommended by the manufacturers. However, treatment using the RTC System was performed by adopting the "stepwise hook extension technique" [21].

The needle was inserted into the tumor percutaneously under sonographic guidance. In the case of RFA, dynamic CT was performed 1–3 days after therapy, and the ablated area was evaluated. The goal of treatment was to obtain an ablative margin larger than the original tumor, with a surrounding treatment margin of 5 mm or greater in all directions. When this margin was not achieved or a residual tumor was found, additional ablation was considered.

In this study, 93 of 131 procedures (71%) were performed using the multitined expandable electrode (LeVeen), 28 of 131 procedures (21%) were performed using the internally cooled electrode (Cool-tip), and 10 of 131 procedures (8%) were performed using the multitined expandable electrode (RITA).

### *Definition of Multinodular Recurrence of HCC*

In this study, we defined "multinodular" as follows: the appearance of 10 or more lesions at the time of first recurrence after surgical resection or RFA.

### *Follow-Up Protocol*

Physicians examined the patients every 4 weeks after treatment, and liver function tests and tumor

**TABLE 1: Clinical Profile and Laboratory Data of 191 Patients With Hepatocellular Carcinoma Treated by Surgical Resection or Radiofrequency Ablation (RFA)**

| Parameter | Surgical Resection | RFA | *p* |
|---|---|---|---|
| Patient characteristics | | | |
| No. of patients | 60 | 131 | |
| Sex (no. of patients) | | | 0.922 |
| M:F ratio | 38:22 | 82:49 | |
| Age (y) | | | 0.021 |
| Median | 66 | 69 | |
| Range | 35–80 | 37–83 | |
| Background liver disease (no. of patients) | | | 0.003 |
| Hepatitis C virus | 34 | 100 | |
| Hepatitis B virus | 22 | 19 | |
| Others | 4 | 12 | |
| Laboratory data | | | |
| Platelet count ($\times 10^4$/μL) | | | 0.153 |
| Median | 13.3 | 11.8 | |
| Range | 5.1–27.2 | 2.7–39.6 | |
| Albumin (g/dL) | | | 0.019 |
| Median | 3.7 | 3.7 | |
| Range | 2.9–4.7 | 2.7–4.4 | |
| Total bilirubin (mg/dL) | | | 0.030 |
| Median | 0.8 | 0.9 | |
| Range | 0.3–2.2 | 0.3–2.7 | |
| Prothrombin activity (%) | | | 0.218 |
| Median | 94.5 | 89.9 | |
| Range | 60.4–124.0 | 56.7–124.0 | |
| AST (IU/L) | | | 0.423 |
| Median | 41 | 48 | |
| Range | 16–163 | 16–191 | |
| AFP (μg/L) | | | 0.561 |
| Median | 12.0 | 10.5 | |
| Range | 1.6–5541.0 | 1.0–993.7 | |
| DCP (AU/L) | | | 0.137 |
| Median | 20.5 | 17.0 | |
| Range | 9.0–556.0 | 6.0–314.0 | |
| Tumor characteristics | | | |
| Diameter (mm) | | | < 0.001 |
| Median | 20.0 | 16.0 | |
| Range | 10.0–30.0 | 7.0–30.0 | |
| Tumor location (no. [%] of patients) | | | |
| Subcapsular | 48/60 (80) | 52/131 (40) | < 0.001 |
| Subphrenic | 24/60 (40) | 58/131 (44) | 0.579 |
| Dynamic CT enhancement pattern (no. [%] of patients) | | | < 0.001 |
| Type 1 | 4 (7) | 46 (35) | |
| Type 2 | 27 (45) | 52 (40) | |
| Type 3 | 21 (35) | 24 (18) | |
| Type 4 | 8 (13) | 9 (7) | |

Note—AFP = α-fetoprotein, AST = aspartate aminotransferase, DCP = des-γ-carboxy prothrombin.

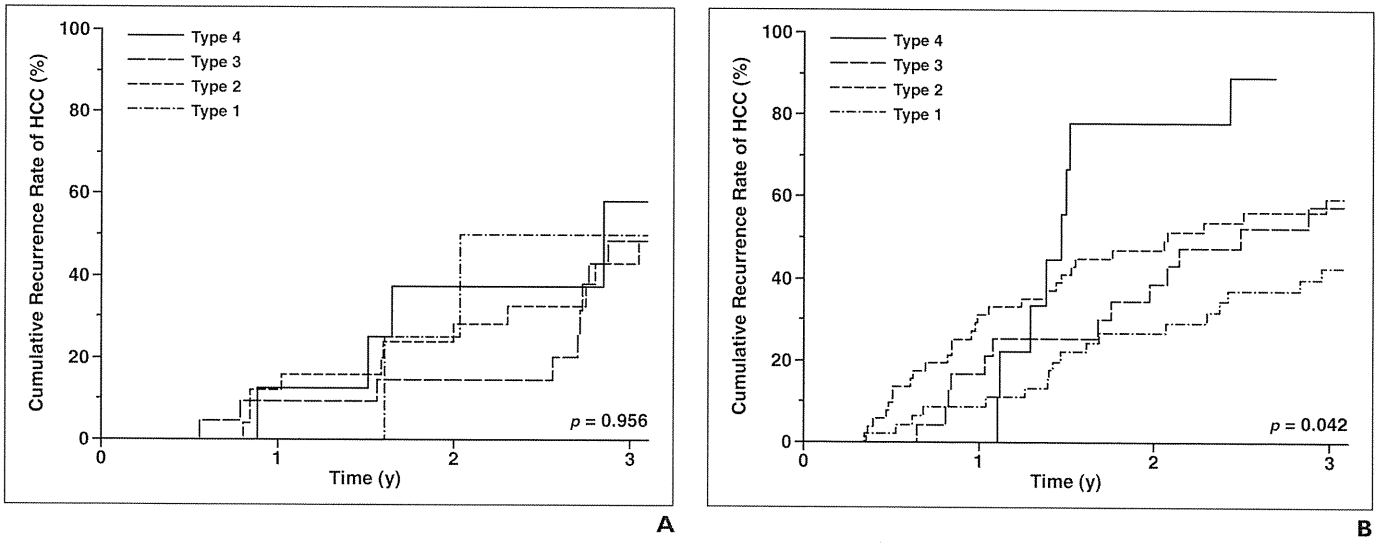


**Fig. 2**—Correlation between cumulative recurrence rates and enhancement patterns of pretreatment dynamic CT after each treatment procedure.
**A** and **B**, Graphs show associations between cumulative hepatocellular carcinoma (HCC) recurrence rate after surgical resection (**A**) and after radiofrequency ablation (**B**) and pretreatment dynamic CT enhancement pattern.

markers were also measured once every month. After completion of HCC treatment, patients underwent contrast-enhanced three-phase CT survey every 3 months for recurrence. Local tumor progression was defined as tumor recurrence adjacent to the resected or ablated area.

### *Statistical Analysis and Ethical Considerations*

Differences in background features and laboratory data between the surgical resection and RFA groups were analyzed by the chi-square test and Mann-Whitney *U* test. Recurrence was analyzed using the Kaplan-Meier technique, and differences in curves were tested using the log-rank test. Independent factors associated with overall recurrence and recurrence characterized by multiple nodules, portal vein invasion, or both were studied using stepwise Cox regression analysis. Potential risk factors for overall recurrence after surgical resection and RFA included the following 15 variables: age, sex, cause of background liver disease, serum albumin level, bilirubin level, aspartate aminotransferase (AST) level, platelet count, prothrombin time, AFP level, des-γ–carboxy prothrombin (DCP) level, diameter of the HCC, tumor location relative to the hepatic capsule (presence or absence of tumor on subcapsular portion), tumor location relative to the diaphragm (presence or absence of tumor on subphrenic portion), treatment procedure, and enhancement pattern of pretreatment dynamic CT analysis.

Potential risk factors for recurrence characterized by multiple nodules, portal vein invasion, or both after RFA included the following 15 variables: age, sex, cause of background liver disease, serum albumin level, bilirubin level, AST level,

**TABLE 2: Predictors of Tumor Recurrence in Patients With Hepatocellular Carcinoma Treated by Surgical Resection or Radiofrequency Ablation (RFA)**

| Category | Univariate Analysis | | Multivariate Analysis | |
|---|---|---|---|---|
| | Hazard Ratio (95% CI) | *p* | Hazard Ratio (95% CI) | *p* |
| Sex | | | | |
| 1: Female | 1 | | | |
| 2: Male | 1.26 (0.84–1.89) | 0.274 | | |
| Age | | | | |
| 1: < 65 y | 1 | | 1 | |
| 2: ≥ 65 y | 1.50 (0.10–2.26) | 0.050 | 1.85 (1.16–2.94) | 0.010 |
| Background liver disease | | | | |
| 1: Hepatitis C virus | 1 | | | |
| 2: Hepatitis B virus | 0.84 (0.51–1.39) | 0.503 | | |
| 3: Others | 1.29 (0.66–2.49) | 0.458 | | |
| Platelet count | | | | |
| 1: ≥ 10 ´ $10^4$/μL | 1 | | 1 | |
| 2: < 10 ´ $10^4$/μL | 1.65 (1.10–2.49) | 0.016 | 1.61 (1.04–2.48) | 0.033 |
| Albumin | | | | |
| 1: ≥ 3.5 g/dL | 1 | | | |
| 2: < 3.5 g/dL | 1.72 (1.15–2.58) | 0.008 | | |
| Total bilirubin | | | | |
| 1: < 1.0 mg/dL | 1 | | | |
| 2: ≥ 1.0 mg/dL | 1.64 (1.11–2.42) | 0.013 | | |
| Prothrombin activity | | | | |
| 1: ≥ 70% | 1 | | | |
| 2: < 70% | 1.95 (1.01–3.75) | 0.046 | | |
| AST | | | | |
| 1: < 40 IU/L | 1 | | 1 | |
| 2: ≥ 40 IU/L | 1.65 (1.09–2.49) | 0.018 | 1.66 (1.04–2.66) | 0.035 |

**(Table 2 continues on next page)**

**TABLE 2: Predictors of Tumor Recurrence in Patients With Hepatocellular Carcinoma Treated by Surgical Resection or Radiofrequency Ablation (RFA) (continued)**

| Category | Univariate Analysis | | Multivariate Analysis | |
|---|---|---|---|---|
| | Hazard Ratio (95% CI) | p | Hazard Ratio (95% CI) | p |
| AFP | | | | |
| 1: < 100 μg/L | 1 | | 1 | |
| 2: ≥ 100 μg/L | 2.21 (1.40–3.50) | 0.001 | 2.25 (1.30–3.89) | 0.004 |
| DCP | | | | |
| 1: < 30 AU/L | 1 | | 1 | |
| 2: ≥ 30 AU/L | 1.82 (1.15–2.88) | 0.011 | 1.77 (1.05–2.99) | 0.032 |
| Tumor diameter | | | | |
| 1: < 20 mm | 1 | | | |
| 2: ≥ 20 mm | 1.13 (0.76–1.67) | 0.544 | | |
| Tumor on subcapsular portion | | | | |
| 1: Yes | 1 | | 1 | |
| 2: No | 1.37 (0.93–2.00) | 0.115 | 1.72 (1.10–2.70) | 0.019 |
| Tumor on subphrenic portion | | | | |
| 1: No | 1 | | | |
| 2: Yes | 1.01 (0.68–1.49) | 0.984 | | |
| Treatment | | | | |
| 1: Surgical resection | 1 | | | |
| 2: RFA | 1.52 (0.98–2.36) | 0.062 | | |
| Dynamic CT enhancement pattern | | | | |
| 1: Type 1 | 1 | | | |
| 2: Type 2 | 1.33 (0.81–2.18) | 0.261 | | |
| 3: Type 3 | 1.15 (0.66–2.01) | 0.628 | | |
| 4: Type 4 | 1.95 (0.98–3.89) | 0.058 | | |

Note—AFP = α-fetoprotein, AST = aspartate aminotransferase, DCP = des-γ-carboxy prothrombin.

platelet count, prothrombin time, AFP level, DCP level, tumor diameter, tumor location relative to capsule (subcapsular portion), tumor location relative to diaphragm (subphrenic portion), type of RFA device, and dynamic CT enhancement pattern. Several variables were transformed into categoric data consisting of two to four simple ordinal numbers for univariate and multivariate analyses. All factors that were at least marginally associated with overall recurrence and recurrence characterized by multiple nodules, portal vein invasion, or both ($p < 0.15$) in univariate analysis were entered into a stepwise Cox regression analysis. Significant variables were selected by the stepwise method. A two-tailed $p < 0.05$ was considered to be statistically significant. Data analysis was performed using statistics software (SPSS, version 11.0, SPSS Inc.).

The study protocol was approved by the Human Ethics Review Committee of Toranomon Hospital.

## Results

### *Clinical Background, Laboratory Data, and Distribution of Enhancement Patterns on Pretreatment Dynamic CT*

Table 1 summarizes the clinical profile and laboratory data of 191 HCC patients who were treated by surgical resection or RFA. The RFA group included significantly older individuals and significantly more patients with less preserved liver function compared with the surgical resection group. The cause of background liver disease was also significantly different between the two treatment groups: Patients in the surgical resection group had larger tumors that were more likely to have a subcapsular location.

The type 2, 3, and 4 enhancement patterns were more commonly observed in the surgical resection group than the type 1 enhancement pattern. In contrast, in the RFA group, the type 1 enhancement pattern was more commonly observed than the type 2, 3, or 4 pattern. In addition, the distribution of enhancement patterns on pretreatment dynamic CT was significantly different for each treatment procedure.

### *Distribution of Each Enhancement Pattern and Frequency of Poorly Differentiated Hepatocellular Carcinoma by Histologic Examination in the Surgical Resection Group*

In 60 surgical resection patients, four patients (7%) had the type 1 enhancement pattern, 27 patients (45%) had the type 2 pattern, 21 patients (35%) had the type 3 pattern, and eight patients (13%) had the type 4 pattern. Pathologic HCC diagnoses by enhancement pattern were as follows: type 1 enhancement pattern, all patients had well-differentiated HCC; type 2 enhancement pattern, five of 27 patients (19%) had well-differentiated HCC and 21 of 27 (78%) patients had moderately differentiated HCC; type 3 enhancement pattern, one of 21 patients (5%) had well-differentiated HCC and 19 of 21 (90%) patients had moderately differentiated HCC; and type 4 enhancement pattern, five of eight patients (63%) had moderately differentiated HCC. Rates of poorly differentiated HCC by enhancement pattern were as follows: type 1 enhancement pattern, zero of four patients (0%); type 2 enhancement pattern, one of 27 patients (4%); type 3 enhancement pattern, one of 21 patients (5%); and type 4 enhancement pattern, three of eight patients (38%).

### *Correlation Between Cumulative Recurrence Rates and Enhancement Patterns on Pretreatment Dynamic CT After Each Treatment Procedure*

In the surgical resection group, cumulative recurrence rates were not significantly different between each pretreatment dynamic CT enhancement pattern (types 1, 2, 3, and 4: 0.0%, 12.0%, 9.5%, and 12.5% at the first year after treatment, respectively, and 25.0%, 28.2%, 14.6%, and 37.5% at the second year) (Fig. 2A). However, in the RFA group, the cumulative recurrence rate was significantly different between each enhancement pattern (types 1, 2, 3, and 4: 8.7%, 31.1%, 16.7%, and 0.0% at the first year, respectively, and 26.6%, 46.9%, 38.6%, and 77.8% at the second year, respectively; $p = 0.042$) (Fig. 2B).

### *Predictive Factors for Initial Recurrence After Surgical Resection or Radiofrequency Ablation*

Multivariate Cox proportional hazards analysis revealed that the following independent

factors are predictive for recurrence of HCC treated by surgical resection or RFA: AFP ≥ 100 μ g/L (hazard ratio [HR], 2.25; 95% CI, 1.30–3.89; $p$ = 0.004), age ≥ 65 years (HR, 1.85; 95% CI, 1.16–2.94; $p$ = 0.010), DCP ≥ 30 AU/L (HR, 1.77; 95% CI, 1.05–2.99; $p$ = 0.032), tumor not present in subcapsular portion (HR, 1.72; 95% CI, 1.10–2.70; $p$ = 0.019), AST ≥ 40 IU/L (HR, 1.66; 95% CI, 1.04–2.66; $p$ = 0.035), and platelet count < $10 \times 10^4$/μL (HR, 1.61; 95% CI, 1.04–2.48; $p$ = 0.033) (Table 2).

### *Association Between the Frequency of Recurrence Characterized by Multiple Nodules, Portal Vein Invasion, or Both and Clinical Features for Each Treatment Procedure*

The frequency and clinical features of recurrence characterized by multiple nodules, portal vein invasion, or both are presented in Table 3. Such recurrences occurred in 10 of 191 patients (5.2%). In the surgical resection group, recurrence occurred in one of 60 patients (1.7%), and in the RFA group, recurrence occurred in nine of 131 patients (6.9%). Notably, in the RFA group, six of nine patients (66.7%) had a pretreatment type 4 enhancement pattern. Among the type 4 patients, recurrence of HCC occurred more than 1 year after treatment in six of six patients (100%) after RFA.

Regarding the needles used for RFA of HCC in these nine patients, an internally cooled electrode (Cool-tip) was used in case 2 (Table 3), a RITA multitined expandable electrode was used in case 4, and a LeVeen multitined expandable electrode was used in the other seven patients.

Figure 3 shows a case of recurrence after RFA (case 7 in Table 3). Figures 3A and 3B show that the pretreatment dynamic CT and digital subtraction angiography (DSA) images revealed a type 4 dynamic CT enhancement pattern. In Figures 3C and 3D, dynamic CT and DSA images acquired at the time of recurrence after RFA are shown: Multiple hepatic tumors are apparent surrounding the previously ablated area.

### *Association Between Cumulative Hepatocellular Carcinoma Recurrence Rate After Radiofrequency Ablation and Pretreatment Dynamic CT Enhancement Patterns: Type 4 Versus Other Enhancement Patterns*

In the RFA group, the cumulative recurrence rate was significantly higher in tumors displaying a pretreatment type 4 dynamic CT enhancement pattern than in tumors showing other enhancement patterns (type 4 vs other enhancement patterns, 0.0% vs 2.8% at the first year, 74.6% vs 2.8% at the second year; $p < 0.001$).

### *Predictive Factors for Hepatocellular Carcinoma Recurrences Characterized by Multiple Nodules, Portal Vein Invasion, or Both After Radiofrequency Ablation*

The Multivariate Cox proportional hazards analysis revealed that the type 4 pretreatment dynamic CT enhancement pattern is an independent predictive factor for HCC recurrence characterized by multiple nodules, portal vein invasion, or both in patients with HCC treated by RFA (HR, 27.68; 95% CI, 6.82–112.33; $p < 0.001$) (Table 4).

## Discussion

A number of local eradication therapies are currently available for HCC. However, with the exception of surgical resection, the potential risk of tumor dissemination always exists in patients who receive such therapies. Therefore, to properly select the most suitable therapy for an individual patient, it is important to predict the potential risk of HCC before treatment.

As others have previously reported [17, 18], identification of poorly differentiated HCC is particularly important for making good therapeutic

**TABLE 3: Frequency of Hepatocellular Carcinoma Recurrence Characterized by 10 or More Nodules, Portal Vein Invasion, or Both by Treatment Procedure and Clinical Features**

| Case No. | At the Time of First Treatment[a] | | | | | At the Time of Tumor Recurrence | | | | Survival Period (y) | Patient Status at End of Follow-Up Period |
|---|---|---|---|---|---|---|---|---|---|---|---|
| | Age (y) | Type of Enhancement Pattern | Tumor Diameter (mm) | AFP (μg/L) | DCP (AU/L) | AFP (μg/L) | DCP (AU/L) | Treatment of Recurrence | First Recurrence Period (y) | | |
| 1[b] | 72 | Type 3 | 26 | 3 | 12 | 8 | 14 | Radiation | 2.7 | 4.1 | Alive |
| 2[c] | 65 | Type 4 | 9 | 37 | 12 | 34 | 12 | TAI | 1.4 | 1.5 | Dead |
| 3 | 53 | Type 4 | 13 | 117 | 94 | 10 | 978 | TACE and radiation | 1.3 | 2.9 | Alive |
| 4 | 70 | Type 4 | 16 | 3 | 14 | 3 | 10 | TACE | 1.5 | 4.0 | Dead |
| 5 | 77 | Type 4 | 20 | 4 | 33 | 5 | 19 | TACE and RFA | 1.1 | 5.0 | Alive |
| 6 | 60 | Type 4 | 20 | 27 | 32 | 23 | 4313 | TACE | 1.5 | 1.9 | Dead |
| 7 | 83 | Type 4 | 21 | 6 | 34 | 6 | 70 | TACE | 1.5 | 3.0 | Alive |
| 8 | 53 | Type 3 | 10 | 64 | 8 | 141 | 10 | TACE | 0.8 | 4.3 | Alive |
| 9 | 69 | Type 2 | 18 | 55 | 10 | 85 | 16 | TACE | 0.6 | 5.3 | Alive |
| 10 | 73 | Type 2 | 21 | 7 | 12 | 3 | 34 | TACE | 0.8 | 4.0 | Alive |

Note—AFP = α-fetoprotein, DCP = des-γ-carboxy prothrombin, TACE = transcatheter arterial chemoembolization, and TAI = transcatheter arterial infusion chemotherapy. RFA = radiofrequency ablation.

[a]Disease was Child-Pugh class A in all 10 patients.

[b]For surgical resection, advanced recurrence occurred in one of 60 patients (1.7%) (case 1).

[c]For RFA, advanced recurrence occurred in nine of 131 patients (6.9%) (cases 2–10).

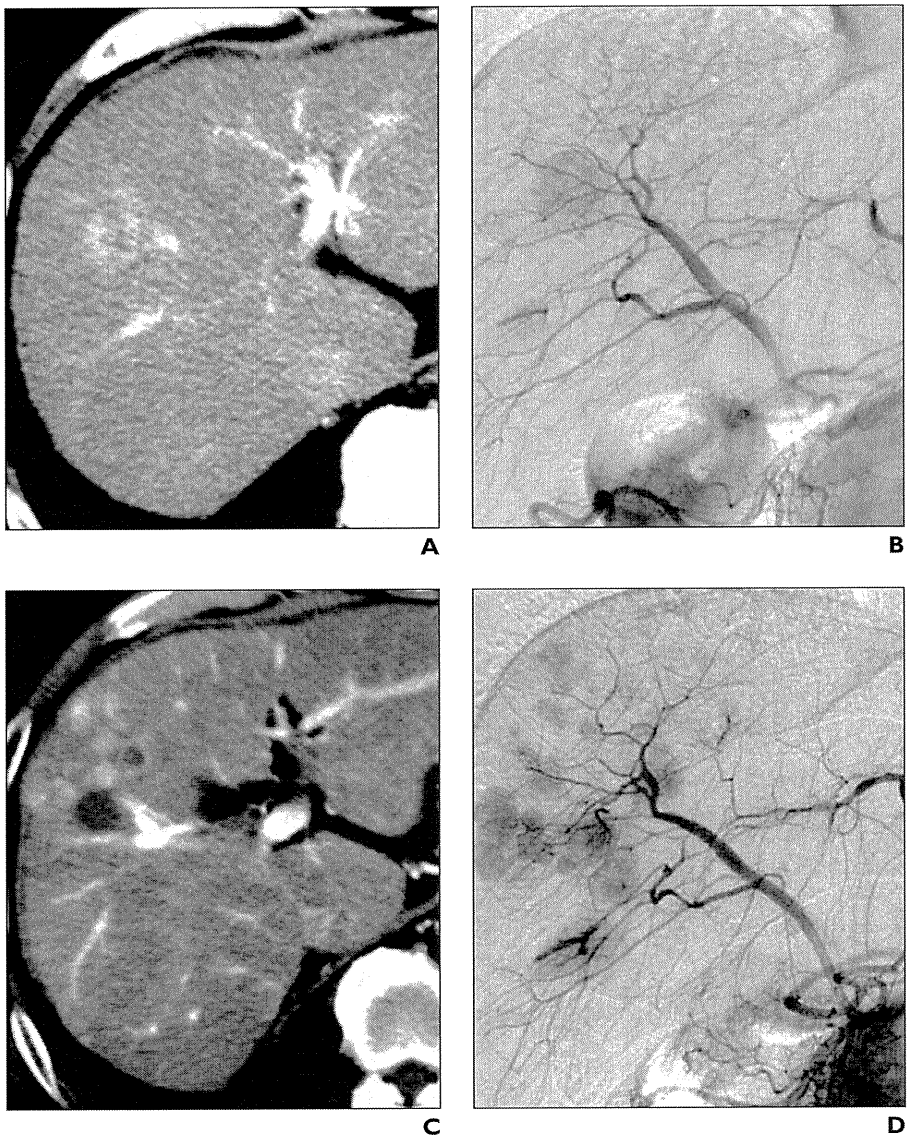


**Fig. 3**—83-year-old man with hepatocellular carcinoma (case 7 in Table 3).
**A,** Pretreatment dynamic CT (arterial phase) image. Tumor shows heterogeneous enhancement pattern with irregular ringlike structures—that is, type 4 enhancement pattern.
**B,** Pretreatment digital subtraction angiography (DSA) image shows single hypervascular nodule, so radiofrequency ablation (RFA) was performed.
**C,** Dynamic CT study (arterial phase) image obtained at time of recurrence after RFA (1.5 years after treatment) shows multiple hepatic tumors are observed around previously ablated area.
**D,** DSA image at time of recurrence shows multiple hepatic tumors are observed around original tumor.

progress. In one of our previous studies, we identified the type 4 enhancement pattern as an independent factor that is predictive of poorly differentiated HCC [19]. The results of that study revealed that the risk of a pathologic diagnosis of poorly differentiated HCC in patients with a preoperative type 4 dynamic CT enhancement pattern is approximately 13 times higher than that of patients with a type 1 or 2 enhancement pattern.

Therefore, the first aim of this study was to evaluate the clinical outcomes of patients with HCC treated by surgical resection and of those with HCC treated by RFA in association with dynamic CT enhancement patterns. In the surgical resection group, no significant differences in recurrence rates were observed between patients with different enhancement patterns. We presume that no significant differences were observed because surgical resection is the most effective local eradication therapy for HCC. In contrast, in the RFA group, significant differences in recurrence rates were observed between patients with different enhancement patterns. This result is surmised to reflect the association between each enhancement pattern and histopathologic diagnosis based on the results of these associations in the surgical resection group. However, in multivariate analysis, pretreatment dynamic CT enhancement pattern was not identified as an independent factor predictive for recurrence of HCC. Therefore, a larger-scale examination is required in the future; depending on the results of that study, it may be necessary to reclassify these enhancement patterns.

The second aim of this study was to investigate the relationship between recurrence characterized by 10 or more nodules, portal vein invasion, or both and pretreatment dynamic CT enhancement pattern in the RFA group. Significant differences between the enhancement patterns and recurrence rates were observed, and in multivariate analysis, a pretreatment type 4 dynamic CT enhancement pattern was identified as an independent factor predictive of this type of HCC recurrence after RFA treatment. The risk of this type of recurrence in patients with a pretreatment type 4 dynamic CT enhancement pattern was approximately 28 times higher than that of other enhancement patterns. Based on these results, this new classification of dynamic CT enhancement pattern—particularly the type 4 enhancement pattern—appears to be very useful for avoiding RFA treatment likely to recur.

In addition, among the six patients with a pretreatment type 4 dynamic CT enhancement pattern who underwent RFA, this type of HCC recurrence occurred more than 1 year after treatment in all six patients (100%). Histopathologic tumor features and adhesion molecules may have contributed to this long interval between the initial treatment and this type of recurrence after RFA. However, in this study, we were not able to perform tumor biopsies of nodules in patients with the type 4 enhancement pattern. Further studies, including histopathologic and molecular biologic examinations, are required to confirm this hypothesis.

This study has some limitations. First, there were more HCC patients with HCV in the RFA group than in the surgical resection group; this difference might have been a potential source of bias. This difference may be because patients with HBV-related HCC usually have a better liver reserve than those with HCV-related HCC at the time of initial hepatocarcinogenesis and that patients with

**TABLE 4: Predictors of Recurrence Characterized by Multiple Nodules, Portal Vein Invasion, or Both in Patients With Hepatocellular Carcinoma Who Underwent Radiofrequency Ablation (RFA)**

| Category | Univariate Analysis | | Multivariate Analysis | |
|---|---|---|---|---|
| | Hazard Ratio (95% CI) | *p* | Hazard Ratio (95% CI) | *p* |
| Sex | | | | |
| 1: Female | 1 | | | |
| 2: Male | 0.50 (0.14–1.87) | 0.305 | | |
| Age | | | | |
| 1: < 65 y | 1 | | | |
| 2: ≥ 65 y | 1.31 (0.33–5.24) | 0.703 | | |
| Background liver disease | | | | |
| 1: Hepatitis C virus | 1 | | | |
| 2: Hepatitis B virus | 0.41 (0.05–3.30) | 0.405 | | |
| 3: Others | 1.23 (0.15–9.87) | 0.843 | | |
| Platelet count | | | | |
| 1: ≥ 10 ´ $10^4$/μL | 1 | | | |
| 2: < 10 ´ $10^4$/μL | 0.58(1.17–2.86) | 0.499 | | |
| Albumin | | | | |
| 1: ≥ 3.5 g/dL | 1 | | | |
| 2: < 3.5 g/dL | 1.22 (0.30–4.88) | 0.783 | | |
| Total bilirubin | | | | |
| 1: < 1.0 mg/dL | 1 | | | |
| 2: ≥ 1.0 mg/dL | 1.36 (0.36–5.06) | 0.649 | | |
| Prothrombin activity | | | | |
| 1: ≥ 70% | 1 | | | |
| 2: < 70% | 2.04 (0.25–16.39) | 0.505 | | |
| AST | | | | |
| 1: < 40 IU/L | 1 | | | |
| 2: ≥ 40 IU/L | 4.99 (0.62–39.93) | 0.130 | | |
| AFP | | | | |
| 1: < 100 μg/L | 1 | | | |
| 2: ≥ 100 μg/L | 1.01 (0.13–8.02) | 0.998 | | |
| DCP | | | | |
| 1: < 30 AU/L | 1 | | | |
| 2: ≥ 30 AU/L | 3.73 (1.00–13.89) | 0.050 | | |
| Tumor diameter | | | | |
| 1: < 20 mm | 1 | | | |
| 2: ≥ 20 mm | 1.62 (0.43–6.03) | 0.473 | | |
| Tumor on subcapsular portion | | | | |
| 1: Yes | 1 | | | |
| 2: No | 2.44 (0.50–11.11) | 0.272 | | |
| Tumor on subphrenic portion | | | | |
| 1: No | 1 | | | |
| 2: Yes | 1.60 (0.43–5.96) | 0.484 | | |
| Type of RFA needle | | | | |
| 1: LeVeen Needle Electrode[a] (Boston Scientific Japan) | 1 | | | |
| 2: Cool-tip[b] (Covidien) | 0.46 (0.06–3.75) | 0.470 | | |
| 3: Model 1500 series[a] (RITA Medical Systems) | 1.36 (0.17–11.05) | 0.774 | | |
| Type of enhancement pattern | | | | |
| 1: Types 1, 2, and 3 | 1 | | 1 | |
| 2: Type 4 | 29.52 (7.28–119.82) | < 0.001 | 27.68 (6.82–112.33) | < 0.001 |

Note—AFP = α-fetoprotein, AST = aspartate aminotransferase, DCP = des-γ-carboxy prothrombin.
[a]Multitined expandable electrode.
[b]Internally cooled electrode.

HCV-related HCC generally have smaller tumors than those with HBV-related HCC. Thus, more patients with HCV-related HCC were treated by RFA. Another limitation is that diagnosis of HCC was essentially based on image analysis, and heterogeneous enhancement resembling the type 4 enhancement pattern is recognized in other hepatic tumors (e.g., cholangiocellular carcinoma and fibrolamellar HCC). However, these other tumors that show the type 4 enhancement pattern are rare in patients with chronic hepatitis or liver cirrhosis compared with HCC: Cholangiocellular carcinoma comprises 4.4% of primary liver cancers [22] and fibrolamellar HCC represents only 0.68% of liver tumors in Japan. Thus, detection of a heterogeneous enhancement pattern on dynamic CT images should be considered first to represent HCC with a highly malignant potential. Moreover, regarding HCC nodules that have a type 4 enhancement pattern, MRI (T1- and T2-weighted images, contrast-enhanced MRI, and comparison of diffusion-weighted images obtained with different b values) is considered to contribute to improved tumor characterization. Adoption of these advanced techniques is expected to increase moving forward.

In our opinion, in patients with a type 4 enhancement pattern on dynamic CT images who have adequate liver reserve to allow any treatment, including surgical resection, we believe that the information about recurrence in this population could be used as an index to prioritize surgical resection. If surgical resection cannot be performed, we recommend up-front embolic therapies (e.g., TACE, radioembolization) rather than RFA monotherapy alone.

In conclusion, the current study showed a strong relationship between the type 4 enhancement pattern and HCC recurrence characterized by 10 or more nodules, portal vein invasion, or both after RFA treatment. The management of HCC with a type 4 enhancement pattern should include a thorough therapeutic approach including surgical resection.

## References


1. El-Serag HB, Mason AC. Rising incidence of hepatocellular carcinoma in the United States. *N Engl J Med* 1999; 340:745–750
2. Bosch X, Ribes J, Borràs J. Epidemiology of primary liver cancer. *Semin Liver Dis* 1999; 19:271–285
3. Okuda K, Fujimoto I, Hanai A, Urano Y. Changing incidence of hepatocellular carcinoma in Japan. *Cancer Res* 1987; 47:4967–4972
4. Johnson PJ, Williams R. Cirrhosis and the aetiology of hepatocellular carcinoma. *J Hepatol* 1987; 4:140–147
5. Ikeda K, Saitoh S, Koida I, et al. A multivariate analysis of risk factors for hepatocellular carcinogenesis: a prospective observation of 795 patients with viral and alcoholic cirrhosis. *Hepatology* 1993; 18:47–53
6. Poon RT, Fan ST, Lo CM, et al. Hepatocellular carcinoma in the elderly: results of surgical and nonsurgical management. *Am J Gastroenterol* 1999; 94:2460–2466
7. Yamanaka N, Okamoto E, Toyosaka A, et al. Prognostic factors after hepatectomy for hepatocellular carcinomas: a univariate and multivariate analysis. *Cancer* 1990; 65:1104–1110
8. Kawasaki S, Makuuchi M, Miyagawa S, et al. Results of hepatic resection for hepatocellular carcinoma. *World J Surg* 1995; 19:31–34
9. Shirabe K, Kanematsu T, Matsumata T, Adachi E, Akazawa K, Sugimachi K. Factors linked to early recurrence of small hepatocellular carcinoma after hepatectomy: univariate and multivariate analyses. *Hepatology* 1991; 14:802–805
10. Jwo SC, Chiu JH, Chau GY, Loong CC, Lui WY. Risk factors linked to tumor recurrence of human hepatocellular carcinoma after hepatic resection. *Hepatology* 1992; 16:1367–1371
11. Nagasue N, Kohno H, Hayashi T, et al. Lack of intratumoral heterogeneity in DNA ploidy pattern of hepatocellular carcinoma. *Gastroenterology* 1993; 105:1449–1454
12. Izumi R, Shimizu K, Ii T, et al. Prognostic factors of hepatocellular carcinoma in patients undergoing hepatic resection. *Gastroenterology* 1994; 106:720–727
13. Otto G, Heuschen U, Hofmann WJ, Krumm G, Hinz U, Herfarth C. Survival and recurrence after liver transplantation versus liver resection for hepatocellular carcinoma: a retrospective analysis. *Ann Surg* 1998; 227:424–432
14. Takayama T, Makuuchi M, Hirohashi S, et al. Early hepatocellular carcinoma as an entity with a high rate of surgical cure. *Hepatology* 1998; 28:1241–1246
15. Zhang BH, Yang BH, Tang ZY. Randomized controlled trial of screening for hepatocellular carcinoma. *J Cancer Res Clin Oncol* 2004; 130: 417–422
16. Hong SN, Lee SY, Choi MS, et al. Comparing the outcomes of radiofrequency ablation and surgery in patients with a single small hepatocellular carcinoma and well-preserved hepatic function. *J Clin Gastroenterol* 2005; 39:247–252
17. Llovet JM, Vilana R, Brú C, et al. Increased risk of tumor seeding after percutaneous radiofrequency ablation for single hepatocellular carcinoma. *Hepatology* 2001; 33:1124–1129
18. Yu HC, Cheng JS, Lai KH, et al. Factors for early tumor recurrence of single small hepatocellular carcinoma after percutaneous radiofrequency ablation therapy. *World J Gastroenterol* 2005; 11: 1439–1444
19. Kawamura Y, Ikeda K, Hirakawa M, et al. New classification of dynamic computed tomography images predictive of malignant characteristics of hepatocellular carcinoma. *Hepatol Res* 2010; 40: 1006–1014
20. Bruix J, Sherman M; Practice Guidelines Committee, American Association for the Study of Liver Diseases. Management of hepatocellular carcinoma. *Hepatology* 2005; 42:1208–1236
21. Kobayashi M, Ikeda K, Someya T, et al. Stepwise hook extension technique for radiofrequency ablation therapy of hepatocellular carcinoma. *Oncology* 2002; 63:139–144
22. Ikai I, Kudo M, Arii S, et al. Report of the 18th follow-up survey of primary liver cancer in Japan. *Hepatol Res* 2010; 40:1043–1059

NEOPLASIA
www.neoplasia.com

Volume 13 Number 3 March 2011 pp. 187–197 **187**

# Metronomic S-1 Chemotherapy and Vandetanib: An Efficacious and Nontoxic Treatment for Hepatocellular Carcinoma[1]

**Hideki Iwamoto[*,†], Takuji Torimura[*,†], Toru Nakamura[*,†], Osamu Hashimoto[*,†], Kinya Inoue[*,†], Junichi Kurogi[*], Takashi Niizeki[*], Reiichiro Kuwahara[*], Mitsuhiko Abe[*], Hiromori Koga[*], Hirohisa Yano[‡], Robert S. Kerbel[§], Takato Ueno[*,†] and Michio Sata[*]**

*Division of Gastroenterology, Department of Medicine, Kurume University School of Medicine, Kurume, Japan; †Research Center for Innovative Cancer Therapy, Kurume University School of Medicine, Kurume, Japan; ‡Department of Pathology, Kurume University School of Medicine, Kurume, Japan; §Molecular and Cellular Biology Research Sunnybrook Health Sciences Centre, Toronto, Ontario, Canada

## Abstract

*BACKGROUND:* Metronomic chemotherapy involves frequent, regular administration of cytotoxic drugs at nontoxic doses, usually without prolonged breaks. We investigated the therapeutic efficacies of metronomic S-1, an oral 5-fluorouracil prodrug, and vandetanib, an epidermal growth factor receptor and vascular endothelial growth factor (VEGF) receptor tyrosine kinase inhibitor, in models of hepatocellular carcinoma (HCC). *METHODS:* We compared anti-HCC effects and toxicity in the six treatment groups: control (untreated), maximum tolerated dose (MTD) S-1, metronomic S-1, vandetanib, MTD S-1 with vandetanib, and metronomic S-1 with vandetanib. Tumor microvessel density (MVD) and tumor apoptosis were evaluated by immunohistochemistry. The expression of VEGF and thrombospondin-1, an endogenous inhibitor of angiogenesis, was analyzed by Western blot. *RESULTS:* Metronomic S-1 significantly inhibited tumor growth, which was enhanced by combination with vandetanib. With respect to toxicities, MTD S-1 caused severe body weight loss and myelosuppression, whereas metronomic S-1 did not cause any overt toxicities. Moreover, metronomic S-1 or metronomic S-1 with vandetanib prolonged survival, the latter treatment providing the greatest benefit. Metronomic S-1 and metronomic S-1 with vandetanib decreased MVDs and increased apoptosis in tumor tissues. The expression of VEGF in tumor tissues was upregulated by vandetanib and metronomic S-1 with vandetanib, whereas the expression of thrombospondin-1 was upregulated by metronomic S-1 and metronomic S-1 with vandetanib. *CONCLUSION:* Metronomic S-1 with an antiangiogenic agent seems to be an effective and safe therapeutic strategy for HCC.

*Neoplasia (2011) 13, 187–197*

## Introduction

Hepatocellular carcinoma (HCC) is the fifth most common solid tumor and the third leading cause of cancer-related deaths globally [1]. Although prognosis of early and intermediate stage HCC has improved owing to advances in treatments, there are few proven effective systemic therapies for advanced HCC [2]. In particular, conventional chemotherapy using cytotoxic drugs for advanced HCC has not been shown to improve survival. Almost all cases of HCC occur in patients with chronic liver disorders, such as liver cirrhosis. Patients with liver cirrhosis have liver dysfunction and also pancytopenia. These pathologies

Abbreviations: HCC, hepatocellular carcinoma; MTD, maximum tolerated dose; MVD, microvessel density; VEGF, vascular endothelial growth factor; EGF, epidermal growth factor; TSP-1, thrombospondin-1; HUVEC, human umbilical vascular endothelial cell

Address all correspondence to: Hideki Iwamoto, MD, Division of Gastroenterology, Department of Medicine, Kurume University School of Medicine, 67 Asahi-Machi, Kurume-shi, Fukuoka-ken, 830-0011, Japan. E-mail: iwamoto_hideki@med.kurume-u.ac.jp

[1]All authors agreed to the submission of this article, and there is no conflict to disclose.

Received 18 August 2010; Revised 6 December 2010; Accepted 8 December 2010

 1522-8002/11/$25.00
DOI 10.1593/neo.101186

limit the use of conventional chemotherapy as a treatment strategy for HCC.

Conventional chemotherapy often involves pulsatile administration schedules using maximum tolerated doses (MTDs) of cytotoxic drugs. The long break periods between therapies not only allow recovery from various toxicities, especially myelosuppression, but also provide an opportunity, unfortunately, for the drug-treated tumors to recover as well [3]. In contrast, metronomic chemotherapy is given at frequent intervals using minimally or nontoxic doses without prolonged breaks. In several preclinical studies, such metronomic protocols have shown surprisingly effective antitumor effects, despite the reduced toxicity [4–6].

S-1 is an orally novel cytotoxic 5-flurouracil (5-FU) prodrug, which consists of tegafur and two biochemical modulators, 5-chloro-2,4-dihydroxypyridine and potassium oxonate [7]. 5-Chloro-2,4-dihydroxypyridine competitively inhibits dihydropyrimidine dehydrogenase approximately 180 times more effectively than uracil. Thus, S-1 gives rise to high concentrations of 5-FU in blood and tumor tissue for long-term periods since biochemical modulation [7,8]. A drug similar to S-1, namely, UFT, has been used successfully in metronomic preclinical studies [5]. Moreover, in the clinic it has been used successfully in randomized phase 3 trials in a metronomic fashion to treat in an adjuvant manner a variety of early stage cancers, after surgery, including non–small cell lung cancer [9] and breast cancer [10]. Because S-1 is thought to be more potent than UFT with respect to the effect of biochemical modulations, one might expect a stronger antitumor effect by using S-1 [7]. In this study, we describe a method of administering metronomic S-1 to treat HCC and compare it to conventional MTD S-1 chemotherapy, either alone or with an antiangiogenic drug.

Tyrosine kinase inhibitors such as sorafenib have proven activity in HCC patients and now represent one of the few effective systemic therapies for HCC [11]. Preclinical studies have also shown that the antitumor effect of metronomic chemotherapy can be significantly enhanced by combination with vascular endothelial growth factor (VEGF) pathway targeting agents [12,13]. In this study, we show here that metronomic S-1 might be a promising therapy to consider for concurrent daily combination with an oral antiangiogenic drug, in this case, vandetanib (ZD6474; AstraZeneca Pharmaceuticals, Macclesfield, UK). Vandetanib inhibits not only the catalytic function of VEGFR-2 but also EGF receptors (EGFRs), in contrast to sorafenib or sunitinib that do not affect EGFRs [14]. We evaluated the efficacies of vandetanib alone *in vivo* for HCC-bearing mice using various hepatoma cell lines that had different expressions of EGFR (submitted for publication). EGFR is known to contribute to 5-FU drug resistance, and 5-FU is the major metabolite of S-1 [15]. Therefore, there is a rationale for drug targeting of both EGF receptors and VEGF receptors along with metronomic chemotherapy, which was the purpose of this study. Thus, we investigated the efficacy of combining with each treatment schedule of S-1 and vandetanib using two HCC cell lines, which express low or high levels of EGFR, that is, KYN-2 and Huh-7, respectively. Overall, our results suggest that the combination treatment of metronomic S-1 plus vandetanib may be useful for the therapy of HCC.

## Materials and Methods

### *Cell Lines and Culture*

In human hepatoma cell lines, Huh-7 was originally purchased from CAMBREX Bio Science Walkersville, Inc (Walkersville, MD), and KYN-2 was provided by the Department of Pathology, Kurume University School of Medicine. Cells were maintained in Dulbecco modified Eagle medium (DMEM; Gibco Invitrogen Cell Culture Co, Auckland, New Zealand) supplemented with 10% fetal bovine serum (FBS).

Human umbilical vascular endothelial cells (HUVECs) were purchased from CAMBREX Bio Science Walkersville, Inc, and maintained with endothelial cell growth medium-2 (Clonetics, San Diego, CA) containing 5% FBS.

### *Animals and Drugs*

Male 5-week-old nude mice (BALB/c *nu/nu*) were purchased from Kyudo KK (Fukuoka, Japan). All experiments were conducted in accordance with the National Institutes of Health guidelines for the Care and Use of Laboratory Animals.

5-FU was purchased from Kyowa Hakko Kogyo Co, Ltd (Tokyo, Japan). S-1 was provided by Taiho Pharmaceutical Co, Ltd (Tokyo, Japan). S-1 consists of a mixture of tegafur, gimeracil, and oteracil at molar ratio of 1:0.4:1 in 0.5% hydroxypropylmethylcellulose (HPMC) solutions. Vandetanib (ZD6474; Zactima) was provided by AstraZeneca Pharmaceuticals (Macclesfield, UK).

### In Vitro *Cell Proliferation Assay*

As the tegafur component of S-1 is physiologically converted to 5-FU in the body, we evaluated the difference of antiproliferative effects *in vitro* of 5-FU using different schedules with both hepatoma cells and HUVECs. Approximately 1000 cells in 100 μl of DMEM containing 10% FBS was added to each well of 96-well plate. After incubation for 24 hours, the medium was exchanged to the serum-containing medium with various concentrations of 5-FU (0, 1, 10, 100, 500, 1000, 10,000 ng/ml). Each cell line was exposed to 5-FU for 5 days. To evaluate the antiproliferative effect of "MTD" *versus* "metronomic" chemotherapy, exchange of the medium containing 5-FU was performed using different schedules. For the metronomic schedule, the medium containing 5-FU was exchanged daily as described previously [16]. For the MTD schedule, the medium containing 5-FU was not changed. After incubation, cell proliferation was evaluated by a tetrazolium-based assay (Cell Count Reagent SF; Nakalai Tesque, Inc, Kyoto, Japan).

### *Determination of the Optimal Dose for S-1 Using Metronomic Chemotherapy*

We determined the optimal metronomic dose of S-1 according to a previous report, which involved evaluating different doses of a chemotherapy drug both for antitumor effects and toxicity, with the aim of determining a dose that has minimal toxicity but retains good efficacy [17]. A total of $5 \times 10^6$ Huh-7 cells were injected into the flank regions of nude mice. Therapy with different doses of S-1 was initiated when the estimated tumor volume ($0.52 \times \text{length} \times \text{width}^2$) reached 150 to 200 $mm^3$. Mice received S-1 orally administrated by gavage with the following agents on a daily basis for 14 days: 1) HPMC as the control group; 2) S-1, 7.5 mg/kg per day; 3) S-1, 5.0 mg/kg per day; 4) S-1, 2.5 mg/kg per day; or 5) S-1, 1.0 mg/kg per day. Tumor-bearing mice were randomly divided into groups of 10 mice. The mice were killed at day 15 after start of treatment. The inhibition rate of tumor growth (IR %) was calculated as follows: IR % = (1 − mean RTV of treatment group / mean RTV of control group) × 100, where RTV indicates the relative tumor volume: tumor volume on killing / tumor volume on initial treatment. For comparison of the toxicity in each group, mouse body weights were measured every 3 days. Peripheral leukocyte count and hemoglobin (Hb) concentrations of these mice were also measured at day 15.

### *Tumor Growth and Toxicity Assessment in the Subcutaneous Tumor Transplant Model*

We selected as the optimal metronomic dosage for S-1, 5.0 mg/kg per day based on our aforementioned study. We selected the MTD for S-1 15 mg/kg per day for 7 days, followed by a 7-day break period, based on previous published findings [6]. To compare the antitumor effect and toxicity caused by MTD or metronomic S-1, long-term experiments were performed using the Huh-7 subcutaneous transplant model. Mice were randomly divided to six groups: 1) HPMC as the control group; 2) MTD S-1, 15 mg/kg per day p.o. for 1 week, followed by a 1-week break period for a cumulative dose of 95 mg/kg; 3) metronomic S-1, 5 mg/kg per day p.o. for 2 weeks without any break period for a cumulative dose of 70 mg/kg; 4) vandetanib 25 mg/kg per day p.o. for 2 weeks; 5) MTD S-1 with vandetanib; or 6) metronomic S-1 with vandetanib. Each group consisted of 10 mice. It is important to note that the cumulative metronomic doses were distinctly less than the cumulative MTD. In other words, whereas the schedule used was "dose-dense," it was not "dose intense." The aforementioned schedules were performed in two cycles, 4 weeks in total. Estimated tumor volumes were measured every 3 days, and all mice were killed after 4 weeks of treatment. For comparison of the toxicity in each group, mouse body weights were measured every 3 days. Peripheral leukocyte count and hemoglobin (Hb) concentrations in these mice were also measured at sacrifice.

### *Tumor Growth and Survival Assessment in the Orthotopic Transplant Model*

We also examined tumor growth using an orthotopic liver transplant model. The mice were implanted with $2 \times 10^6$ KYN-2 cells into the left lobe liver. Mice were randomly divided into six groups, as outlined above, and therapy was initiated 7 days after implantation of tumor cells. Each group consisted of 10 mice. The mice were killed at day 29 of initial treatment, and tumor volumes were evaluated.

In addition, a survival study was also performed using the KYN-2 orthotopic transplant model for the six groups as mentioned above. Each group consisted of 10 mice. In the group for survival observation, animals were killed according to (pre)clinical signs of weakness, for example, anorexia, or greater than 20% weight loss, and days of life were recorded from initial treatment.

### *Immunohistochemical Staining of CD31, PCNA, and TUNEL*

The sections of all tumor tissues obtained from KYN-2 orthotopic transplant model were boiled for 30 minutes by high pH target retrieval solution (DAKO Japan, Kyoto, Japan) for antigen retrieval. The sections were incubated with rabbit anti–human CD31 antibody (diluted 1:300; Abcam, Inc, Tokyo, Japan) and rabbit anti–human PCNA antibody (diluted 1:250; Abcam, Inc) at 4°C overnight. Then the avidin-biotin procedures were subsequently performed using a Vectastatin ABC Kit (Vector Laboratories, Inc, Burlingame, CA). The sections were reacted with 0.005% $H_2O_2$–3,3′-diaminobenzidine at room temperature for 1 minute. For quantification of microvessel density (MVD), CD31-positive vessels were counted in randomly selected 30 areas per five tumors in each treatment group at 200-fold magnification.

The terminal deoxynucleotidyl transferase–mediated dUTP nick end labeling (TUNEL) method was performed for the evaluation of apoptosis in each of the treated tumor tissues. TUNEL labeling was performed using the ApopTag Kit (Chemicon, Temecula, CA) according to the manufacturer's instructions. The stained sections of tumors of each group were reviewed, and the apoptosis index, determined by TUNEL staining, was determined by counting at least 1000 cells in five randomly selected high-power fields (magnification, ×200).

### *Expression of Thrombospondin-1 and VEGF in Tumor Tissues*

We examined the expression of VEGF and thrombospondin-1 (TSP-1) in treated tumor tissues using Western blot analysis. TSP-1 is a known endogenous antiangiogenic protein [18]. Five samples of each treatment group and control group were loaded in equal conditions, respectively. Thirty micrograms of protein was loaded onto a NuPAGE 4% to 12% Bis-Tris gel (Invitrogen, CA). Membranes were incubated with rabbit anti–TSP-1 antibody (1:350 dilution; Abcam, Inc) or rabbit anti-VEGF antibody (1:500 dilution; Abcam, Inc) at 4°C overnight. Equal protein loading was assessed by mouse anti–β-actin antibody (1:1000 dilution; Sigma, St Louis, MO). After incubation with HRP-conjugated anti–rabbit immunoglobulin G (1:10,000 dilution; GE Healthcare UK Ltd, Buckinghamshire, UK) or HRP-conjugated anti–mouse immunoglobulin G antibody (1:5000 dilution; GE Healthcare UK Ltd) for 1 hour, immunoreactive bands were stained by an enhanced chemiluminescence Western blot analysis system using LAS 4000 mini (Fujifilm, Tokyo, Japan) and were calculated with the amount of luminescence in each sample using multigauge software (Fujifilm). The relative amount of luminescence in each treatment group for the control group was expressed as [(treatment group VEGF or TSP-1 / treatment group β-actin) / (control group VEGF or TSP-1 / control group β-actin)] and compared with each group.

### *Statistical Analysis*

All experimental data were expressed as mean ± SD. Differences between groups were examined for statistical significance using the Mann-Whitney *U* test, the Kruskal-Wallis test, and nonparametric analysis of variance. If the one-way analysis of variance was significant, differences between individual groups were estimated using the Fisher least significant difference test. Overall survival was estimated according to the Kaplan-Meier method and compared using the log-rank test. $P < .05$ was considered to be statistically significant.

## Results

### *Comparison of Antiproliferative Effects of Metronomic versus MTD Type Chemotherapy* In Vitro

The 50% inhibitory concentration ($IC_{50}$) levels of metronomic and MTD schedules of 5-FU, the major metabolite of S-1, for each cell line are shown in Table 1. The antiproliferative effects of 5-FU for each cell line were found to be dose-dependent (Figure 1, *A–C*). The $IC_{50}$ levels for the MTD and metronomic schedule for Huh-7 cells were 3.84 and 0.77 μM, respectively (Figure 1*A*). The $IC_{50}$

**Table 1.** $IC_{50}$ Levels of MTD and Metronomic Schedule in Hepatoma Cell Lines and Endothelial Cell.

| | 5-FU $IC_{50}$ (μM) | |
|---|---|---|
| | MTD | Metronomic |
| Hepatoma cell lines | | |
| Huh-7 | 3.84 | 0.77 |
| KYN-2 | 7.69 | 3.84 |
| Endothelial cell | | |
| HUVECs | 7.7 | 0.76 |

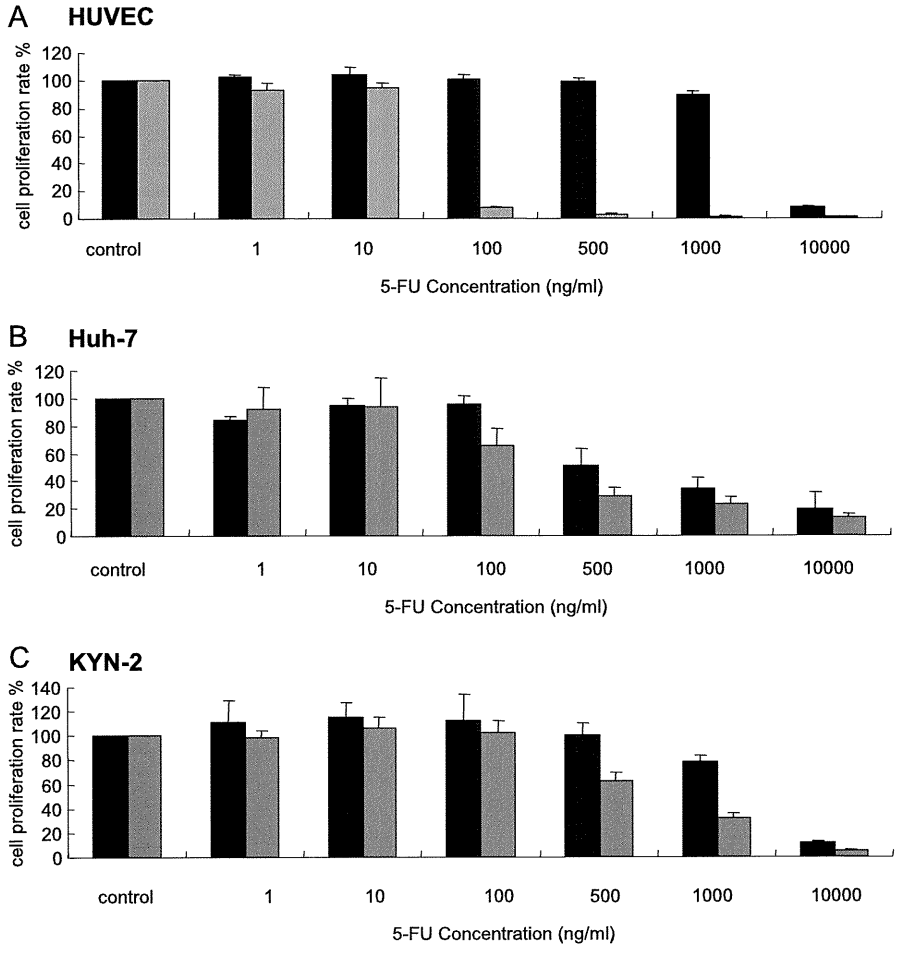


**Figure 1.** Inhibitory effect of metronomic chemotherapy for each cell line tested in a cell proliferation assay. To evaluate the antiproliferative effect of "MTD" and "metronomic" chemotherapy *in vitro*, exchange of the medium containing 5-FU was performed in different schedules. For the metronomic schedule, the medium containing 5-FU (0, 1, 10, 100, 500, 1000, and 10,000 ng/ml) was exchanged once a day. For the MTD schedule, the medium containing 5-FU was not changed. Data are shown as a ratio of the control and expressed as mean ± SD of 10 samples. *$P < .001$ compared with each schedule. Dark gray–shaded columns show MTD schedule, and light gray–shaded columns showed metronomic schedule. (A) HUVEC. HUVEC was cultured with 100 $\mu$l of endothelial cell growth medium-2 with 5% FBS containing 5-FU. (B) Huh-7. (C) KYN-2. Hepatoma cells were cultured with 100 $\mu$l of DMEM with 10% FBS containing 5-FU.

levels for KYN-2 were 7.69 and 3.84 μM, respectively. For the hepatoma cell lines, the metronomic schedule inhibited cell proliferation at approximately 1/2 to 1/4 concentrations of 5-FU compared with MTD schedule (Table 1). The metronomic schedule for HUVECs inhibited cell proliferation at apparently lower levels ($IC_{50}$ levels, 0.76 μM) approximately 1/10 the concentration of 5-FU compared with MTD schedule ($IC_{50}$ levels, 7.7 μM; Table 1).

### *Determination of the Optimal Dose of S-1 for Metronomic Chemotherapy* In Vivo*: Maximum Tumor Growth Inhibition with Minimal Toxicity*

In the 7.5- and 5.0-mg/kg-per-day S-1 treatment groups, there were significant differences in suppression of tumor growth compared with the control group ($P < .05$; Figure 2*A*), and dosages lower than 2.5 mg/kg per day S-1 were not statistically effective compared with the control group. In addition, we evaluated body weight loss and myelosuppression toxicities associated with administration of S-1 (Figure 2, *B–D*). With respect to body weight loss, there was no significant difference between each group (Figure 2*B*). But only the 7.5-mg/kg-per-day group showed severe toxicity as determined by reductions in Hb concentration and leukocyte count ($P < .001$, compared with the control group; Figure 2, *C* and *D*). Therefore, we selected 5.0 mg/kg per day as the optimal metronomic dosage of S-1, which was used in all subsequent experiments.

### *Evaluation of the Antitumor Effect and Toxicity for Metronomic S-1 Chemotherapy in the Subcutaneous Transplant Tumor Model*

In the assay for tumor growth, statistical differences were observed between the control group and all treatment groups (Figure 3*A*).

Metronomic S-1 potently inhibited tumor growth compared with MTD S-1 ($P < .01$). The mean tumor volumes were 4810.5 ± 1440.9 $cm^3$ in the control group, 3212.6 ± 1364.7 $cm^3$ in the MTD S-1 group, 1927.1 ± 652.9 $cm^3$ in the metronomic S-1 group, and 2331.4 ± 662.1 $cm^3$ in the vandetanib group, respectively. The mean tumor volumes in the MTD S-1 plus vandetanib group and metronomic S-1 plus vandetanib group were 2026.7 ± 1106.7 and 1383.7 ± 697.5 $cm^3$, respectively. The greatest inhibition of tumor growth was induced by the metronomic S-1 in combination with vandetanib (Figure 3*A*). In addition, we evaluated toxicity in each of Huh-7 subcutaneous tumor treatment groups (Figure 3, *B–D*). In leukocyte count, there were no significant differences in the groups (Figure 3*B*). In Hb concentration, the control group was 12.84 ± 1.82 g/dl, the MTD S-1 group was 9.77 ± 3.63 g/dl, the metronomic S-1 group was 11.73 ± 3.27 g/dl, and the vandetanib group was 12.34 ± 2.77 g/dl. For the combination treatments, the MTD S-1 plus vandetanib group was 8.24 ± 1.64 g/dl, and for the metronomic S-1 plus vandetanib group, it was 11.74 ± 1.55 g/dl (Figure 3*C*). With respect to rate of body weight loss, in the MTD S-1 monotherapy and MTD S-1 with vandetanib groups, the values observed were 10.48% ± 6.85% and 8.59% ± 5.02% reduction compared with the control group, respectively. Vandetanib, metronomic S-1, and the combination therapy resulted in 5.64% ± 4.23%, 3.04% ± 2.23%, and −0.51% ± 5.56% reduction compared with the control group, respectively (Figure 3*D*). Both the MTD S-1 and MTD S-1 plus vandetanib treatment groups experienced severe body weight loss and reduced Hb concentrations compared with the control group (Figure 3, *C* and *D*). In marked contrast, the metronomic S-1 monotherapy and metronomic S-1 with vandetanib groups did not manifest any overt toxicity (Figure 3, *B–D*).

### *Evaluation of Antitumor Efficacy Using Metronomic S-1 Chemotherapy in an Orthotopic Liver Transplant Model*

For tumor volume assessments, all treatments except MTD S-1 monotherapy were effective compared with the control group (Figure 4*A*). Tumor volumes at sacrifice were 4186.0 ± 1128.0 $cm^3$ in the control group, 3259.0 ± 788.7 $cm^3$ in the MTD S-1 group, 1501.3 ± 1002.2 $cm^3$ in the metronomic S-1 group, and 1582.0 ± 354.9 $cm^3$ in the vandetanib group. There was a significant difference between metronomic S-1 and MTD S-1 in tumor growth inhibition ($P < .05$; Figure 4*A*). For the combination treatment groups, tumor volumes were 931.1 ± 331.7 $cm^3$ in the MTD S-1 plus vandetanib group and 875.0 ± 369.4 $cm^3$ in the metronomic S-1 plus vandetanib group. There was no significant difference between the metronomic S-1 plus vandetanib group and the MTD S-1 plus vandetanib group. However, the greatest inhibition of tumor growth was detected in the metronomic S-1 plus vandetanib treatment group ($P < .001$; Figure 4*A*).

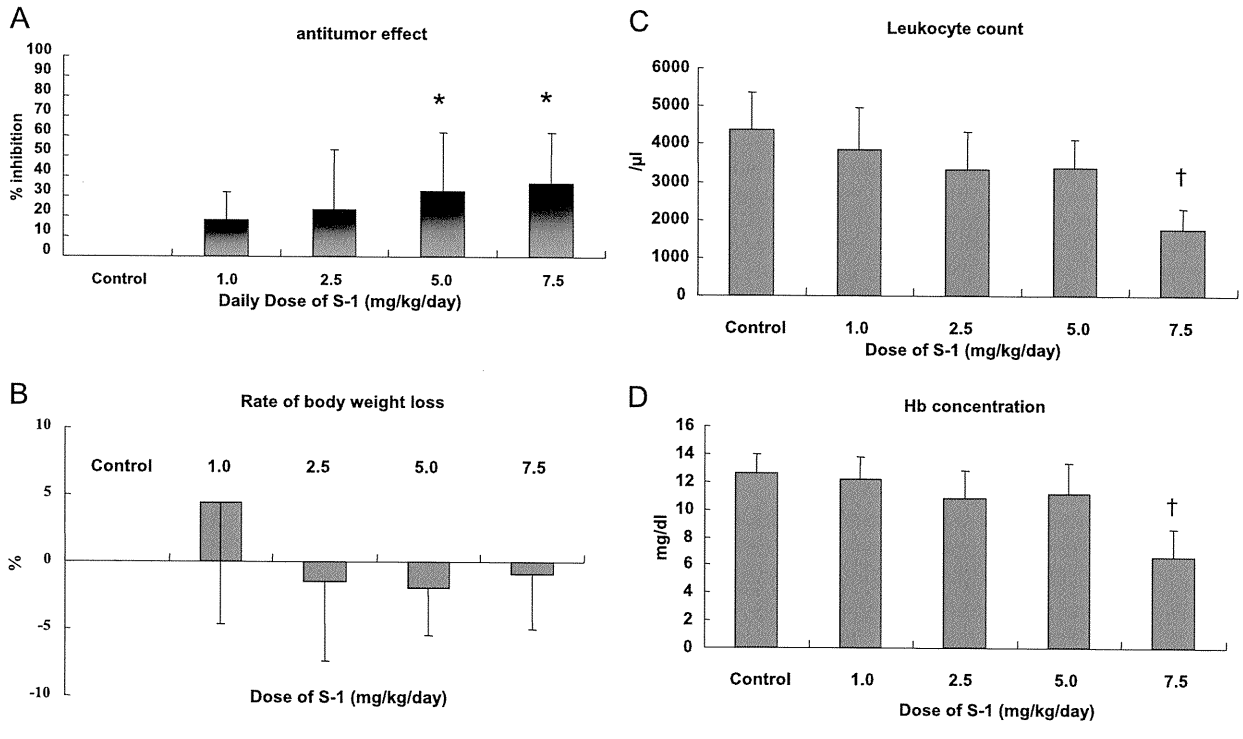


**Figure 2.** Determination of the optimal dose of S-1 in metronomic chemotherapy. Huh-7 subcutaneous tumor models were treated daily with either HPMC or different metronomic doses of S-1 (1.0, 2.5, 5.0, or 7.5 mg/kg per day) for 14 consecutive days. (A) Inhibition rates of tumor volumes (%) are expressed as mean ± SD ($n = 10$ per group). Dosages of 5.0 and 7.5 mg/kg per day S-1 groups statistically inhibited tumor growth compared with the control group (*$P < .05$). (B–D) Toxicity parameters are represented as mean ± SD. (B) Body weight (BW) changes on killing were calculated according to the following formula: BW change (%) = [(BW on sacrifice) − (BW on day 0)] × 100. (C) Hb concentration. (D) Leukocyte count. Each different dose of S-1 did not show body weight loss. However, the only 7.5-mg/kg-per-day S-1 group represented severe myelosuppression, such as decreased Hb concentration or leukocyte count. †$P < .001$ by compared with the control group.

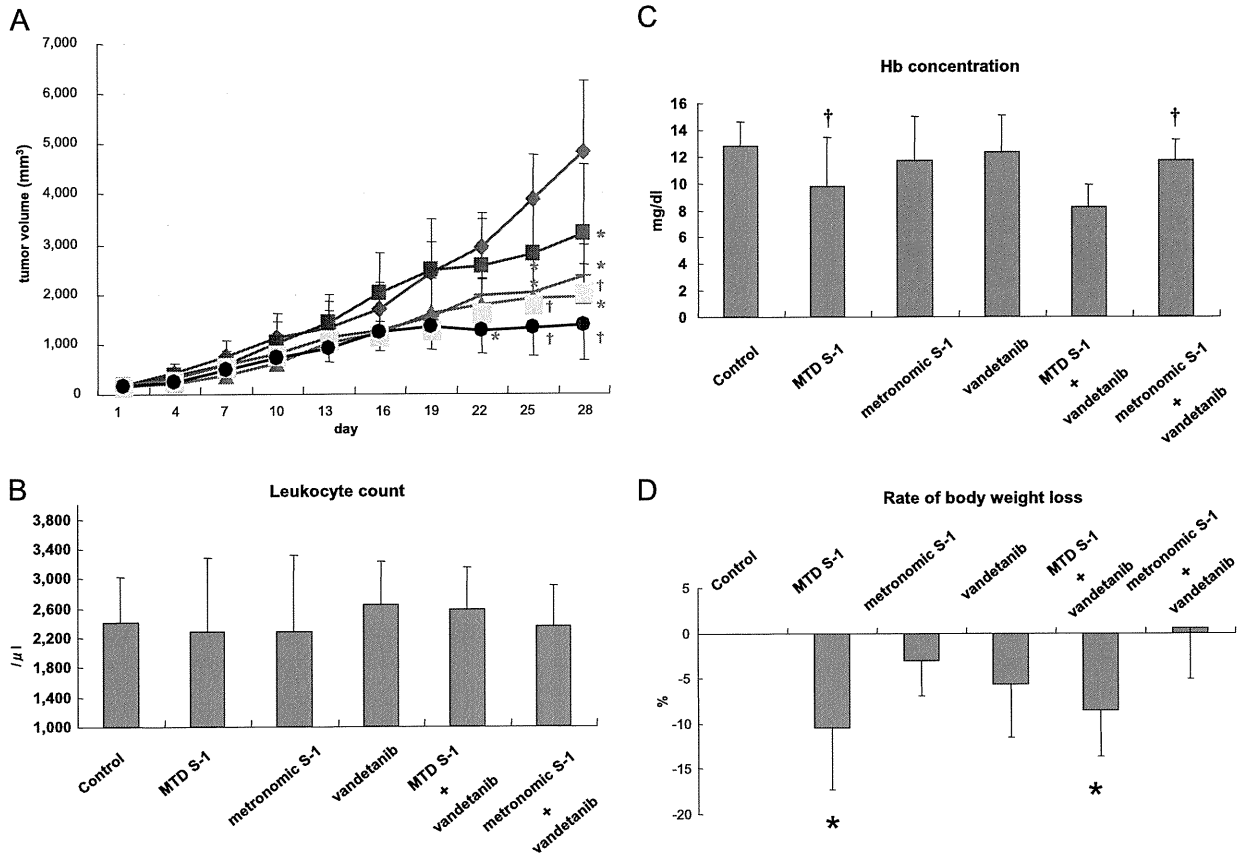


**Figure 3.** Therapeutic effects of metronomic S-1 chemotherapy in the Huh-7 subcutaneous tumor transplant model. (A) Tumor-bearing nude mice ($n$ = 10 per group) were treated in the following six groups: 1) HPMC as the control group (blue); 2) MTD S-1 15 mg/kg per day for 1 week, followed by a 1-week break period (purple); 3) metronomic S-1 5 mg/kg per day for 2 weeks without break period (green); 4) vandetanib 25 mg/kg per day for 2 weeks (red); 5) MTD S-1 with vandetanib (yellow); or 6) metronomic S-1 with vandetanib (black). All treatments were performed for 4 weeks in total. Tumor volume changes are expressed as mean ± SD. All treatments showed efficacy compared with the control group (*$P$ < .05), and the metronomic S-1 therapy was more effective than the MTD S-1 treatment. The metronomic S-1 with vandetanib significantly inhibited tumor growth compared with the control group (†$P$ < .001). (B–D) Toxicity parameters are expressed as mean ± SD. (B) Hb concentration. (C) Leukocyte count. (D) Rate of body weight loss. MTD S-1 and the MTD S-1 with vandetanib showed severe body weight loss (*$P$ < .01) and decreased Hb concentration (†$P$ < .05) compared with the control group. Metronomic S-1 and the metronomic S-1 with vandetanib did not show any overt toxicities.

### *Evaluation of Survival Using Metronomic S-1 Chemotherapy in an Orthotopic Liver Transplant Model*

The mean survival time in the control group was 28.9 ± 6.4 days. MTD S-1 did not prolong survival (mean survival time, 29.6 ± 3.9 days). In contrast, metronomic S-1 significantly prolonged survival (mean survival time, 34.3 ± 4.8 days). The mean survival time in the vandetanib group was 33.6 ± 5.0 days. MTD S-1 plus vandetanib treatment did not prolong survival times compared with vandetanib monotherapy (mean survival time, 37.6 ± 5.5 days). However, the metronomic S-1 plus vandetanib group provided the greatest prolonged survival times among all the treatment groups (mean survival time, 49.6 ± 11.5 days; Figure 4*B*).

### *Effect of Metronomic S-1 Chemotherapy Alone and in Combination with Vandetanib on Parameters of Tumor Angiogenesis*

The results in Figure 5 show the MVD count in each treatment group. There was no significant difference in the MVD count between the control and the MTD S-1 group (control 41.1 ± 9.2, MTD S-1 35.8 ± 5.5; Figure 5*B*). However, tumor MVD was decreased in the metronomic S-1 group (17.2 ± 4.1) compared with the control group ($P$ < .001) and the MTD S-1 group ($P$ < .001; Figure 5*B*). Tumor MVD in mice treated with vandetanib was 13.7 ± 5.1. In the MTD S-1 plus vandetanib group, the MVD count was 18.8 ± 7.4. Metronomic S-1 plus vandetanib group showed the greatest reduction of tumor MVD ($P$ < .01 compared with MTD S-1 plus vandetanib group, 8.2 ± 1.6; Figure 5*B*).

### *Detection of Proliferation and Apoptotic Cells in Tumor Tissues*

To further investigate the mechanism of the observed antitumor effect, we examined the effect of metronomic S-1 and in combination with vandetanib on tumor cell proliferation and apoptosis (Figure 5). With respect to tumor cell proliferation, there were no differences between the control and all treated groups. The mean